



**HAL**  
open science

## Smooth particle methods without smoothing

Martin Campos Pinto

► **To cite this version:**

| Martin Campos Pinto. Smooth particle methods without smoothing. 2011. hal-00649821v1

**HAL Id: hal-00649821**

**<https://hal.science/hal-00649821v1>**

Preprint submitted on 8 Dec 2011 (v1), last revised 6 Nov 2014 (v2)

**HAL** is a multi-disciplinary open access archive for the deposit and dissemination of scientific research documents, whether they are published or not. The documents may come from teaching and research institutions in France or abroad, or from public or private research centers.

L'archive ouverte pluridisciplinaire **HAL**, est destinée au dépôt et à la diffusion de documents scientifiques de niveau recherche, publiés ou non, émanant des établissements d'enseignement et de recherche français ou étrangers, des laboratoires publics ou privés.

# Smooth particle methods without smoothing

Martin Campos Pinto

CNRS and IRMA (UMR 7501, Université de Strasbourg and CNRS)

December 8, 2011

## Abstract

We present a novel class of particle methods with deformable shapes that achieve high-order convergence rates in the supremum norm. These methods do not require remappings or extended overlapping or vanishing moments for the particles. Unlike classical convergence analysis, our estimates do not rely on a smoothing kernel argument but rather on the uniformly bounded overlapping of the particles supports and on the smoothness of the characteristic flow. In particular, they also apply to heterogeneous “particle approximations” such as piecewise polynomial bases on unstructured meshes. In the first-order case which simply consists of pushing forward linearly transformed particles (LTP) along the flow, we provide an explicit scheme and establish rigorous error estimates that demonstrate its  $L^\infty$  convergence and the uniform boundedness of the particle overlapping. To illustrate the flexibility of the method we also develop an adaptive multilevel version that includes a local correction filter for positivity-preserving hierarchical approximations. Numerical studies demonstrate the convergence properties of this new particle scheme in both its uniform and adaptive versions, and compare it with traditional fixed-shape particle methods with or without remappings.

## 1 Introduction

Efficient and simple particle methods are extremely popular for the numerical simulation of transport equations involved in many physical problems ranging from fluid dynamics [8, 12] to kinetic (e.g., Vlasov) equations [7, 18]. However, particle methods also suffer from weak convergence properties that lead to important disadvantages in many practical cases. Specifically, it is known that they only converge in a strong sense when the particles present an extended overlapping, that is, when the number of overlapping particles tends to infinity as the mesh size  $h$  of their initialization grid tends to 0, see e.g., Refs. [3, 25]. Moreover, convergence rates are known to be suboptimal and for high orders they require additional constraints (namely, vanishing moments) that are not satisfied by positive shape functions. In practice, extended particle overlapping can be expensive and it involves an additional parameter to be optimized, such as the overlapping exponent  $q < 1$  for which the particles radius behaves like  $h^q \gg h$ . In Particle-In-Cell (PIC) codes for instance, this amounts to increasing the number of particles per cell together with the number of cells, as the latter determine the effective radius of the particles [7]. In Smoothed Particle Hydrodynamics (SPH) schemes it amounts to increasing the number of interacting particles [24]. Because of these issues, many particle simulation methods do not meet the conditions of convergence which can result in numerically intensive simulations for acceptable accuracy. Also, limited numerical resources often produce strong oscillations seen as a statistical noise that hamper interpretation of results and can further cause large scale errors.

To suppress noise, many methods (like the Denavit redeposition scheme [16], recently revisited as a Forward Semi-Lagrangian scheme (FSL), see e.g., Refs. [23, 11, 14]) use periodic remappings, i.e., particle re-initializations that smooth out the evolution. However, frequent remappings can introduce unwanted numerical diffusion which leads some authors to introduce high-order adaptive remappings, see, e.g. Refs. [6, 28], and in many cases contradicts the benefit of using low-diffusion particle schemes.

In this article, we present a new class of particle methods with deformable shapes that converge in the supremum norm without requiring remappings or extended overlapping or vanishing moments for the particles. Unlike classical error estimates based on a smoothing kernel argument, our analysis applies to general particle collections with Lipschitz smoothness and bounded overlapping properties. In particular our estimates easily extend to the transport of heterogeneous particle approximations, such as standard finite elements bases.

Our results are threefold. On a formal level first, we establish high-order convergence rates in  $L^\infty$  for a class of transport operators where the particle shapes are deformed with polynomial mappings, the coefficients of which involve spatial derivatives of the backward flow. In particular, the first-order case is a linearly-transformed particle method (LTP) where the particles are deformed with the Jacobian matrices of the backward flow. It corresponds to a method already studied by Cohen and Perthame [10] who established its first-order convergence in  $L^1$  but did not provide a numerical scheme for the deformation matrices. It can also be viewed as a modified version of Hou's method [20] where instead of using a global deformation mapping, each particle is transformed by the linearized flow around its trajectory. On a numerical level, we provide an explicit scheme for the LTP method that is based solely on pointwise evaluations of the forward flow, and we establish rigorous a priori estimates for both the transport error and the particle overlapping. To illustrate the flexibility of our approach we also present an adaptive multilevel LTP scheme where local estimates for the single-particle transport errors are used to decide which particles are dynamically refined, and a local correction filter for high-order positivity-preserving hierarchical approximations is presented. On a practical level we eventually present some academic test cases and show that the LTP scheme converges faster than the traditional "smoothed" particle method with extended overlapping (TSP). Here the convergence is significantly improved by introducing periodic remappings, but compared with the FSL scheme we also show that optimal remapping frequencies are much lower with LTP, leading to lower numerical diffusion and computational cost. Finally we verify that our adaptive LTP scheme enhances the convergence of solutions with sharp edges by equi-distributing the transport error.

As we have pointed out, deforming the particles is not a new idea. Dynamic adaptation, i.e., refinement and coarsening of particles, also has a substantial history. In vortex methods for instance, Cottet, Koumoutsakos and others have introduced a variety of algorithms to handle particles with spatially varying sizes based on global or local mappings, see e.g. [13, 5]. In kinetic (PIC) schemes, Lapenta, Assous and others developed "rezoning" algorithms to increase or lower the number of particles per grid cell, while preserving grid moments such as charge, current or energy density, see e.g. [21, 1]. For pure transport problems, Bergdorf and Koumoutsakos [6] have studied a wavelet-based FSL scheme with adaptive, high-order remappings. However, although the list is not exhaustive we observe that these methods only adapt the size of the particles, and not their shape. A noteworthy exception is the Complex Particle Kinetic method developed by Bateson and Hewett for the simulation of plasmas [2, 19] where in addition to having their Gaussian shape transformed by the local shearing of the flow, the particles can be fragmented to probe for emerging features, and merged where fine particles are no longer needed. When mature, our adaptive scheme will naturally have to be compared with the above methods.

The outline of the article is as follows. In Section 2 we begin with a brief overview of the main particle methods, we introduce some notations and state our main results. In Section 3 we present our class of high-order particle methods with polynomial deformations, and provide a fully discrete LTP scheme with a priori estimates. Section 4 is then devoted to the description of an adaptive multilevel LTP scheme based on refinable B-splines, and our numerical studies are presented in Section 5.

Readers mostly interested in the practical aspects of the LTP scheme may prefer to first read Sections 2.3, 3.1, 3.3 and 3.4. Its main properties are stated in Theorem 3.2, and its adaptive multilevel version is summarized in Algorithms 4.1, 4.2 and 4.4.

## 2 A brief overview of particle methods

To introduce some notations and state our main results we begin with a rapid overview of some important particle methods. Following [25, 10] we consider the linear  $d$ -dimensional transport

equation

$$\partial_t f(t, x) + u(t, x) \cdot \nabla f(t, x) = 0, \quad t \in [0, \tau], \quad x \in \mathbb{R}^d \quad (1)$$

associated with an initial data  $f^{\text{in}} : \mathbb{R}^d \rightarrow \mathbb{R}$ , a final time  $\tau$  and a velocity field  $u : [0, \tau] \times \mathbb{R}^d \rightarrow \mathbb{R}^d$ . In fluid problems for instance, we have  $d = 2, 3$ , while in kinetic formulations  $\mathbb{R}^d$  is a phase space with  $d \leq 6$ , and  $u$  is a generalized velocity field with components of velocity and acceleration. In any case, we assume that  $u$  is smooth enough for the characteristic trajectories  $X(t) = X(t, t_0, x_0)$ , solutions to

$$X'(t) = u(t, X(t)), \quad X(t_0) = x_0, \quad (2)$$

to be defined on  $[0, \tau]$ , for all  $x_0 \in \mathbb{R}^d$  and  $t_0 \in [0, \tau]$ , see, e.g., [25]. In particular, the corresponding characteristic flow  $F_{t_0, t} : x_0 \mapsto X(t)$  is invertible and satisfies  $F_{t, t_0} = (F_{t_0, t})^{-1}$ . Hence solutions to (1) read

$$f(t, x) = f(t_0, (F_{t_0, t})^{-1}(x)) \quad \text{for all } t_0, t \in [0, \tau] \text{ and } x \in \mathbb{R}^d.$$

For simplicity, we restrict ourselves to the incompressible case where  $\text{div } u = 0$ . In particular, the flow is measure preserving in the sense that its Jacobian matrix  $J_{F_{t_0, t}}(x) = (\partial_j (F_{t_0, t})_i)_{1 \leq i, j \leq d}$  has a constant determinant equal to 1,

$$\det (J_{F_{t_0, t}}(x)) = 1 \quad \text{for all } t_0, t \in [0, \tau] \text{ and } x \in \mathbb{R}^d.$$

## 2.1 The traditional smoothed particle method (TSP)

In the standard ‘‘academic’’ particle method [25], numerical solutions are typically computed as follows: considering deterministic initializations for simplicity, the initial data is first approximated by a collection of particles on a regular (say, cartesian) grid of step  $h > 0$ , i.e., we set

$$f_{h, \epsilon}^0(x) := \sum_{k \in \mathbb{Z}^d} w_k(f^{\text{in}}) \varphi_\epsilon(x - x_k) \approx f^{\text{in}}(x), \quad x \in \mathbb{R}^d,$$

with  $x_k = hk$  and weights defined by

$$w_k(f^{\text{in}}) := \int_{x_k + [-\frac{h}{2}, \frac{h}{2}]^d} f^{\text{in}}(x) dx \quad \text{or} \quad w_k(f^{\text{in}}) := h^d f^{\text{in}}(x_k). \quad (3)$$

Here  $\varphi_\epsilon = \epsilon^{-d} \varphi(\cdot/\epsilon)$  is the particle shape function with radius proportional to  $\epsilon$ , usually seen as a smooth approximation of the Dirac measure obtained by scaling a compactly supported ‘‘cut-off’’ function  $\varphi$  for which a common choice is a B-spline. Particle centers are then updated at each time step  $t^n = n\Delta t$  by following the flow  $F^n = F_{t^n, t^{n+1}}$  or its numerical approximation, and the weights are kept constant, leading to

$$f_{h, \epsilon}^{n+1}(x) := \sum_{k \in \mathbb{Z}^d} w_k(f^{\text{in}}) \varphi_\epsilon(x - x_k^{n+1}) \approx f(t^{n+1}, x) \quad \text{with } x_k^{n+1} := F^n(x_k^n), \quad k \in \mathbb{Z}^d,$$

and where we have set  $x_k^0 = x_k$ . In the classical error analysis [3, 25], the above process is seen as (i) an approximation – in the *distribution* sense – of the initial data by a weighted collection of Dirac measures, (ii) the exact transport of the Dirac particles along the flow, and (iii) the smoothing of the resulting distribution  $\sum_k w_k(f^{\text{in}}) \delta_{x_k^n}$  with the convolution kernel  $\varphi_\epsilon$ . The classical error estimate reads then as follows: if for some prescribed integers  $m > 0$  and  $r > 0$ , the cut-off  $\varphi$  has  $m$ -th order smoothness and satisfies a moments condition of order  $r$ , namely if  $\int \varphi = 1$ ,  $\int |x|^r |\varphi(x)| dx < \infty$  and

$$\int x_1^{s_1} \dots x_d^{s_d} \varphi(x_1, \dots, x_d) dx = 0 \quad \text{for } s \in \mathbb{N}^d \text{ with } 1 \leq s_1 + \dots + s_d \leq r - 1,$$

then there exists a constant  $C$  independent of  $f^{\text{in}}, h$  or  $\epsilon$ , such that for all  $n \leq \tau/\Delta t$  we have

$$\|f(t^n) - f_{h, \epsilon}^n\|_{L^\mu} \leq C \left( \epsilon^r \|f^{\text{in}}\|_{W^{r, \mu}} + (h/\epsilon)^m \|f^{\text{in}}\|_{W^{m, \mu}} \right) \quad (4)$$

with  $1 \leq \mu \leq \infty$ . More recently, Cohen and Perthame [10] observed that defining the weights as

$$w_k(f^{\text{in}}) = \int_{\mathbb{R}^d} f^{\text{in}}(x) \tilde{\varphi}_h(x - x_k) dx \quad (5)$$

with weighting function  $\tilde{\varphi}_h = \tilde{\varphi}(\cdot/h)$  derived from a compactly supported  $\tilde{\varphi} \in \mathcal{C}^0(\mathbb{R}^d)$  such that

$$\sum_{k \in \mathbb{Z}^d} k_1^{s_1} \dots k_d^{s_d} \tilde{\varphi}(x - k) = x_1^{s_1} \dots x_d^{s_d} \quad \text{for } s \in \mathbb{N}^d \text{ with } 0 \leq s_1 + \dots + s_d \leq m - 1,$$

one has the improved estimate

$$\|f(t^n) - f_{h,\epsilon}^n\|_{L^\mu} \leq C \left( \epsilon^r \|f^{\text{in}}\|_{W^{r,\mu}} + (h/\epsilon)^m \|f^{\text{in}}\|_{L^\mu} \right) \quad (6)$$

with a new constant that is again independent of  $f^{\text{in}}, h$  or  $\epsilon$ . Note that (6) is better than (4) in that  $m$  is not constrained by the smoothness of  $f^{\text{in}}$ , which allows to reach higher convergence rates. Indeed balancing the error terms in the above estimates suggests to take  $\epsilon \sim h^q$  with  $q = \frac{m}{m+r}$ , yielding a convergence in  $h^{\frac{rm}{m+r}}$ . In particular, if  $f^{\text{in}} \in W^{s,\mu}$  for some integer  $s$  then the best possible rate with standard weights is only  $h^{s/2} \|f^{\text{in}}\|_{W^{s,\mu}}$ , obtained with  $m = r = s$ . With the improved weights instead, one can take a higher value for  $m$  and obtain estimates close to  $h^s \|f^{\text{in}}\|_{W^{s,\mu}}$ . Moreover, the latter approach also allows to improve (i.e., reduce) the particle overlapping, since the corresponding exponents are  $q = \frac{1}{2}$  and  $\frac{m}{m+r} \approx 1$ , respectively. In either case indeed, we see from the term  $h^{qr} \|f^{\text{in}}\|_{W^{r,\mu}}$  in the estimates that extended particle overlapping does not only make the simulations more expensive, it also deteriorates their convergence order.

## 2.2 The forward semi-lagrangian scheme (FSL)

In Forward Semi-Lagrangian schemes (the new name for the periodically remapped particle method introduced by Denavit [16]), extended overlapping is usually not required and particles have the same scale than their initialization grid, i.e.,  $\epsilon = h$ . Instead, their weights and centers are re-initialized on a regular grid once every  $N_r$  time steps. Thus, denoting by

$$A_h : g \mapsto \sum_{k \in \mathbb{Z}^d} w_k(g) \varphi_h(x - x_k)$$

the particle approximation operator with  $x_k = hk$  and weights computed, e.g., as in (3), and by

$$T^n : \varphi_h(\cdot - x_k^n) \mapsto \varphi_h(\cdot - F^n(x_k^n))$$

the fixed-shape particle transport operator, the FSL scheme takes the form

$$f_h^{n+1} := \sum_{k \in \mathbb{Z}^d} w_k^{n+1} \varphi_h(\cdot - x_k^{n+1}) := T^n \tilde{f}_h^n \quad \text{with } \tilde{f}_h^n := \begin{cases} A_h f_h^n & \text{if } \text{mod}(n, N_r) = 0 \\ f_h^n & \text{otherwise,} \end{cases} \quad (7)$$

where  $T^n$  has been extended to collections of particles by linearity.

## 2.3 The linearly-transformed particle method (LTP)

In this article we shall develop a lesser-known approach already studied by Cohen and Perthame [10] who observed that by deforming the particles with the linearized flow around their trajectories, one obtains a convergent method (in  $L^1$ ) with particles scaled with their initialization grid, and no remappings. On a formal level this amounts to defining linearly-transformed particles as

$$\varphi_{h,k}(t, x) := \varphi_h(J_k(t)(x - x_k(t))) \quad \text{with } x_k(t) = F_{0,t}(x_k) \text{ and } J_k(t) := J_{F_{t,0}}(x_k(t)). \quad (8)$$

In practice, we have seen that occasional remappings are needed for accurate solutions. We may then rewrite the numerical LTP scheme in a form similar to (7), but particles are now associated

with invertible  $d \times d$  deformation matrices  $D_k^n$  representing backward Jacobian matrices at  $x_k^n$ . Thus, numerical solutions read

$$f_h^n(x) = \sum_{k \in \mathbb{Z}^d} w_k^n \varphi_{h,k}^n(x) := \sum_{k \in \mathbb{Z}^d} w_k^n \varphi_h(D_k^n(x - x_k^n)) \quad (9)$$

and transporting the particles consists in updating the deformation matrices  $D_k^n$  together with the particle centers  $x_k^n$ . In section 3.3 we will describe a numerical method for doing so, that is solely based on pointwise evaluations of the (approximated) forward flow  $F^n$ . We may then summarize our findings as follows.

**Main results.** *The formal LTP method (8) converges with order 1 in  $L^\infty$ , and arbitrary orders can be reached with proper polynomial deformations which coefficients involve the derivatives of the backward flow (see Theorem 3.1). On the numerical side, an explicit implementation of the LTP transport operator based on finite-difference approximations of the forward Jacobian is also shown to converge with order 1 in  $L^\infty$  with no remappings required (see Theorem 3.2). In practice this leads to improved convergence compared to both TSP and FSL schemes, with lower remapping frequencies than the latter (see Section 5.1). Moreover, local error estimates for the single-particle transport errors are established (see Theorem 3.2 again) that can be used for dynamic refinements in a hierarchical particle framework (see Section 5.2).*

In the sequel it will be convenient to use the maximum norm  $\|x\|_\infty := \max_i |x_i|$  for vectors and the associated  $\|A\|_\infty := \max_i \sum_j |A_{i,j}|$  for matrices. For functions in Sobolev spaces  $W^{m,\infty}(\omega)$  with integer index  $m > 0$  we will use semi-norms defined as

$$|v|_{m,\omega} := \max_i \left\{ \sum_{l_1=1}^d \cdots \sum_{l_m=1}^d \|\partial_{l_1} \cdots \partial_{l_m} v_i\|_{L^\infty(\omega)} \right\},$$

and for conciseness we shall drop the domain  $\omega \subset \mathbb{R}^d$  when it is the whole space.

### 3 Particle methods without smoothing

In this section we develop particle methods that deviate from the existing “smoothed” approaches described in Sections 2.1 and 2.2 in the following sense.

- Convergence (including high-order) is proved without resorting to a smoothing kernel argument as with TSP schemes. Instead particles have their radius proportional to the meshsize  $h$  of their initialization grid, which
  - (i) permits using not only one single particle shape but also heterogeneous collections such as standard finite element bases, as no vanishing moments or high-order smoothness is required ;
  - (ii) allows to compute their weights with standard approximation schemes, including hierarchical ones ;
  - (iii) yields uniformly bounded numbers of overlapping particles.
- Remappings are not required for convergence as in FSL schemes, although they may improve the results in practice.

To simplify the presentation we shall focus on homogeneous spline particles, although heterogeneous bases could be used, see Remark 3.2 below. Thus, in Section 3.1 we first recall one local approximation scheme with B-splines, then in Section 3.2 we introduce the particle transport operators with polynomial shape transformations that converge without smoothing arguments. In Section 3.3 we next describe one explicit implementation of the first-order transport operator  $T_1$ , and after giving one practical tool for localizing arbitrary particles with linearly transformed supports in Section 3.4, we establish rigorous error estimates in Section 3.5, that prove both the uniform convergence and the uniformly bounded overlapping of the deformed particles.

### 3.1 High-order quasi-interpolations with B-spline particles

For simplicity, we shall consider homogeneous particles based on tensorized B-splines. Specifically, the univariate (centered) cardinal B-spline  $\mathcal{B}_p$  is a piecewise polynomial of degree  $p$ , globally  $\mathcal{C}^{p-1}$  and supported on  $[-\frac{p+1}{2}, \frac{p+1}{2}]$ . It can be defined recursively by

$$\mathcal{B}_0 = \chi_{[-\frac{1}{2}, \frac{1}{2}]} \quad \text{and} \quad \mathcal{B}_p(x) = (\mathcal{B}_{p-1} * \mathcal{B}_0)(x) = \int_{x-\frac{1}{2}}^{x+\frac{1}{2}} \mathcal{B}_{p-1}, \quad \text{for } p \geq 1,$$

and its integer translations span the space of cardinal splines of degree  $p$ , see, e.g., [15]. Thus  $\mathcal{B}_1(x) = \max\{1 - |x|, 0\}$  is the traditional hat-function,  $\mathcal{B}_3$  is the centered cubic B-spline, and so on. Specifically, our reference particle shape function will be the tensorized, centered B-spline of odd degree  $p$ ,

$$\varphi(x) = \prod_{i=1}^d \mathcal{B}_p(x_i) \quad \text{supported on} \quad \text{supp}(\varphi) = [-c_p, c_p]^d \quad \text{with } c_p := \frac{p+1}{2}. \quad (10)$$

Note that B-splines of odd degree are refinable, which will later allow us to reformulate our particle method in a hierarchical, multilevel framework.

Since our particles are scaled with their initialization (or remapping) grid, we can use standard approximation schemes that rely on the fact that the span of their integer translates

$$\varphi_{h,k}(x) = \varphi_h(x - x_k) = h^{-d} \varphi(h^{-1}x - k), \quad k \in \mathbb{Z}^d, \quad (11)$$

contains the space  $\mathcal{P}_p$  of polynomials with coordinate degree less or equal to  $p$ . Specifically, we shall consider quasi-interpolation schemes described by [9] and [27], where high-order B-spline approximants are locally obtained by pointwise evaluations of the target function. In the univariate case they take the form

$$A_h^{(1d)} : g \mapsto \sum_{k \in \mathbb{Z}} w_k(g) \varphi_{h,k} \quad \text{with normalized weights} \quad w_k(g) := h \sum_{|l| \leq m_p} a_l g(h(k+l))$$

and symmetric coefficients  $a_l = a_{-l}$  defined in such a way that  $A_h^{(1d)}$  reproduces the space  $\mathcal{P}_p^{(1d)}$ . They can be computed with the iterative algorithm in [9, Section 6]: for the first orders we obtain

- $m_p = 0$  and  $a_0 = 1$  for  $p = 1$ ,
- $m_p = 1$  and  $(a_0, a_1) = (\frac{8}{6}, -\frac{1}{6})$  for  $p = 3$ ,
- $m_p = 4$  and  $(a_0, a_1, a_2, a_3, a_4) = (\frac{503}{288}, -\frac{1469}{3600}, \frac{7}{225}, \frac{13}{3600}, \frac{1}{14400})$  for  $p = 5$ .

In the multivariate case we can tensorize the above, as it is easily checked that the operator

$$A_h : g \mapsto \sum_{k \in \mathbb{Z}^d} w_k(g) \varphi_{h,k} \quad \text{with} \quad w_k(g) := h^d \sum_{\|l\|_\infty \leq m_p} a_l g(h(k+l)) \quad \text{and} \quad a_l := \prod_{1 \leq i \leq d} a_{l_i} \quad (12)$$

reproduces any polynomial  $\pi \in \mathcal{P}_p$ . Moreover, we have

$$\|A_h g\|_{L^\infty} \leq (2c_p)^d \|\varphi_h\|_{L^\infty} \sup_{k \in \mathbb{Z}^d} |w_k(g)| \leq (2c_p)^d \|\varphi\|_{L^\infty} \|a\|_{\ell^1} \|g\|_{L^\infty} \quad (13)$$

with  $\|a\|_{\ell^1} = \sum_{\|l\|_\infty \leq m_p} |a_l|$ , by using the fact that no more than  $(2c_p)^d$  B-splines can overlap. It follows that  $A_h$  is uniformly bounded in  $L^\infty$ , with

$$\|A_h\|_{\mathcal{L}(L^\infty)} := \sup_{g \neq 0} \frac{\|A_h g\|_{L^\infty}}{\|g\|_{L^\infty}} \leq (2c_p)^d \|\varphi\|_{L^\infty} \|a\|_{\ell^1}.$$

In particular, we can localize the above bounds and write, with an integer  $q \leq p$ , that

$$\begin{aligned} \|A_h g - g\|_{L^\infty(B_\infty(x_k, h))} &\leq \inf_{\pi \in \mathcal{P}_q} \{ \|A_h(g - \pi)\|_{L^\infty(B_\infty(x_k, h))} + \|g - \pi\|_{L^\infty(B_\infty(x_k, h))} \} \\ &\leq \inf_{\pi \in \mathcal{P}_q} \{ (\|A_h\|_{\mathcal{L}(L^\infty)} + 1) \|g - \pi\|_{L^\infty(B_\infty(x_k, h(m_p + c_p)))} \} \\ &\leq h^{q+1} (\|A_h\|_{\mathcal{L}(L^\infty)} + 1) \frac{(m_p + c_p)^{q+1}}{(q+1)!} |g|_{q+1, B_\infty(x_k, h(m_p + c_p))} \end{aligned}$$

where  $B_\infty(x, \rho)$  denotes the open cube of center  $x$  and radius  $\rho$ , and where the last inequality is obtained by choosing for  $\pi$  the  $q$ -th Taylor expansion of  $g$  around  $x_k$ , namely  $\pi(x) = \sum_{r=0}^q \frac{1}{r!} \phi^{(r)}(0)$  with  $\phi(s) = g(x_k + s(x - x_k))$ . Hence the high-order global accuracy

$$\|A_h g - g\|_{L^\infty} \leq h^{q+1} c_A |g|_{q+1}, \quad q \leq p \quad (14)$$

with  $c_A = (\|A_h\|_{\mathcal{L}(L^\infty)} + 1) \frac{(m_p + c_p)^{q+1}}{(q+1)!}$ .

### 3.2 High-order particle transport with polynomial shape transformations

We now address the problem of transporting a collection of particles

$$f_h^0 = \sum_{k \in \mathbb{Z}^d} w_k \varphi_{h,k} \approx f^{\text{in}}$$

along the flow  $F = F_{0,\tau}$  associated with the whole time domain, with no remappings. Here we consider particles initially centered on the cartesian grid (11), with weights satisfying

$$|w_k| \leq c_w h^d \|f^{\text{in}}\|_{L^\infty}, \quad k \in \mathbb{Z}^d \quad (15)$$

with a fixed  $c_w > 0$ , as it should be with any standard approximation scheme – if  $f_h^0 = A_h f^{\text{in}}$  this is clearly the case, with  $c_w = \|a\|_{\ell^1}$ . Moreover, to simplify the analysis we begin by forgetting the time discretization (when studying a discrete particle scheme we will take into account the time approximation errors, see Section 3.3 and following) and consider that  $F$  is known and can be applied exactly. Thus, in the traditional method particles keep their shape and are simply translated with

$$T = T_{(0)} : \varphi_{h,k} \mapsto \varphi_h(\cdot - \bar{x}_k), \quad \text{with } \bar{x}_k = F(x_k). \quad (16)$$

Note that the exact transport operator reads

$$T_{\text{ex}} : g \mapsto g(F^{-1}(\cdot)) \quad (17)$$

so that (16) is exact for point (Dirac) particles. For finite-size particles however, the method does not converge: consider the two dimensional case where  $p = 1$ , i.e.,  $\varphi$  is the standard hat function, and the infinitely smooth problem consisting of  $f^{\text{in}} = 1$  and  $u(t, x) = (-x_2, x_1)$  over the time interval  $[0, \frac{\pi}{4}]$ . Then any reasonable initialization will give  $w_k = h^2$ , hence,  $f_h^0(x) = 1$ , and clearly the exact final solution is  $f(\frac{\pi}{4}, x) = 1$ . Now, since at the final time the particle centers will have rotated of  $\tau = \frac{\pi}{4}$ , every particle  $\varphi_{h,k}$  with  $|k_1| + |k_2| = 1$  will be centered on  $(\cos(\theta + \frac{\pi}{4}), \sin(\theta + \frac{\pi}{4}))$  with  $\theta \in \frac{\pi}{2}\mathbb{N}$ , and hence contributes to  $x = 0$  with  $T_{(0)}\varphi_{h,k}(0) = h^{-2}(1 - \frac{1}{\sqrt{2}})^2$ , in addition to  $\varphi_{h,0}$  which does not move. Since other particles do not contribute to  $x = 0$ , the final error satisfies

$$\|(T_{(0)} - T_{\text{ex}})f_h^0\|_{L^\infty} \geq |T_{(0)}f_h^0(0) - f(\frac{\pi}{4}, 0)| = 2(\sqrt{2} - 1)^2, \quad \text{regardless of } h.$$

Now, to improve the accuracy of the transport operator let us analyze its error based on the main property that the transported particles are localized by the relation

$$\text{supp}(T\varphi_{h,k}) \subset \bar{B}_{h,k} := B_\infty(\bar{x}_k, h\bar{\rho}_{h,k}), \quad (18)$$

with radius parameters uniformly bounded by  $\bar{\rho} := \sup_{h>0, k \in \mathbb{Z}^d} \bar{\rho}_{h,k} < \infty$  (which is clearly the case for  $T_{(0)}$ , with  $\bar{\rho}_{h,k} = c_p = \bar{\rho}$ ). Thus, we first observe that if  $T$  is such that (18) holds, then the particles overlap in a bounded way. Indeed for all  $x, k$  such that  $T\varphi_{h,k}(x) \neq 0$  we have  $\|k - h^{-1}F^{-1}(x)\|_\infty \leq h^{-1}|F^{-1}|_1 \|\bar{x}_k - x\|_\infty < \bar{\rho}_{h,k}|F^{-1}|_1$ , hence

$$\sup_{x \in \mathbb{R}^d} \#\{k \in \mathbb{Z}^d : T\varphi_{h,k}(x) \neq 0\} \leq \Theta := (2\bar{\rho}|F^{-1}|_1)^d. \quad (19)$$

Moreover, it is easily seen that the particles transported with the exact operator (17) also satisfy a bounded overlapping: if  $k$  is such that  $T_{\text{ex}}\varphi_{h,k}(x) \neq 0$  then  $\|k - h^{-1}F^{-1}(x)\|_\infty < c_p$ , hence

$$\sup_{x \in \mathbb{R}^d} \#\{k \in \mathbb{Z}^d : T_{\text{ex}}\varphi_{h,k}(x) \neq 0\} \leq \Theta_{\text{ex}} := (2c_p)^d.$$

In particular, we can decompose the global error  $(T - T_{\text{ex}})f_h^0$  in terms of particle transport errors  $e_{h,k} = (T - T_{\text{ex}})\varphi_{h,k}$ , as

$$\|(T - T_{\text{ex}})f_h^0\|_{L^\infty} \leq \Theta_e \sup_{k \in \mathbb{Z}^d} \|w_k(f^{\text{in}})e_{h,k}\|_{L^\infty} \leq h^d c_w \|f^{\text{in}}\|_{L^\infty} \Theta_e \sup_{k \in \mathbb{Z}^d} \|e_{h,k}\|_{L^\infty}$$

holds with  $\Theta_e := \Theta + \Theta_{\text{ex}}$ , where we have used (15). Next we observe that the support of  $T_{\text{ex}}\varphi_{h,k}$  is localized with

$$\begin{aligned} T_{\text{ex}}\varphi_{h,k}(x) \neq 0 &\implies F^{-1}(x) \in \Sigma_{h,k} := \text{supp}(\varphi_{h,k}) = B_\infty(x_k, hc_p) \\ &\implies \|x - \bar{x}_k\|_\infty \leq |F|_{1, \Sigma_{h,k}} \|F^{-1}(x) - x_k\|_\infty < hc_p |F|_{1, \Sigma_{h,k}}, \end{aligned}$$

i.e., we have

$$\text{supp}(T_{\text{ex}}\varphi_{h,k}) = F(\Sigma_{h,k}) = F(B_\infty(x_k, hc_p)) \subset B_\infty(\bar{x}_k, hc_p |F|_{1, \Sigma_{h,k}}). \quad (20)$$

Hence the localization  $\text{supp}(e_{h,k}) \subset \bar{B}_{h,k}^e := B_\infty(\bar{x}_k, h\bar{\rho}_{h,k}^e)$  for the error terms, with a new constant  $\bar{\rho}_{h,k}^e := \max(\bar{\rho}_{h,k}, c_p |F|_{1, \Sigma_{h,k}}) \leq \bar{\rho}^e := \max(\bar{\rho}, c_p |F|_1)$ . In the case of particle translations, i.e., for  $T = T_{(0)}$ , it follows that

$$\begin{aligned} \|e_{h,k}\|_{L^\infty} &= \sup_{x \in \bar{B}_h^e} |\varphi_h(x - \bar{x}_k) - \varphi_h(F^{-1}(x) - F^{-1}(\bar{x}_k))| \\ &\leq |\varphi_h|_1 \sup_{x \in \bar{B}_h^e} \|(F^{-1}(x) - x) - (F^{-1}(\bar{x}_k) - \bar{x}_k)\|_\infty \\ &\leq h^{-d} \bar{\rho}_{h,k}^e |\varphi|_1 |F^{-1} - I|_{1, \bar{B}_{h,k}^e} \end{aligned} \quad (21)$$

where we have used the scaling  $|\varphi_h|_1 \leq h^{-(d+1)}|\varphi|_1$  derived from (11). Thus, by gathering the above steps one finds

$$\|(T_{(0)} - T_{\text{ex}})f_h^0\|_{L^\infty} \leq C \Theta_e \bar{\rho}^e |F^{-1} - I|_1 \|f^{\text{in}}\|_{L^\infty} \quad (22)$$

with a constant  $C$  depending only on  $d, p$ . Note that since  $\det(J_{F^{\pm 1}}(x)) = 1$  is valid for all  $x$ , we have  $1 \leq \|J_{F^{\pm 1}}(x)\|_\infty \leq |F^{\pm 1}|_1$  and hence (22) holds with  $\Theta_e = 2(2|F^{-1}|_1 c_p)^d$  and  $\bar{\rho}^e = c_p |F|_1$ .

Not surprisingly, the above analysis fails short of proving the convergence of particle translations. It also suggests one way to improve their accuracy: setting indeed

$$\phi_k(s) := (F^{-1} - I)(\bar{x}_k + s(x - \bar{x}_k)) \quad (23)$$

we may see the approximation  $(F^{-1}(x) - x) \approx (F^{-1}(\bar{x}_{j,k}) - \bar{x}_k)$  involved in (21) as the zero-order Taylor expansion  $\phi_k(1) \approx \phi_k(0)$ , and hence consider replacing  $\varphi_h(x - \bar{x}_k)$  by  $\varphi_h(\Phi_{k,(r)}(x))$ ,  $r \geq 1$ , where

$$\Phi_{k,(r)}(x) := x - \bar{x}_k + \phi'_k(0) + \dots + \frac{1}{r!} \phi_k^{(r)}(0) \approx F^{-1}(x) - x_k \quad (24)$$

is formally an  $r$ -th order approximation. Note that one could also consider expansions of the alternate  $\tilde{\phi}_k(s) := (I - F)(x_k + s(F^{-1}(x) - x_k))$  since  $\tilde{\phi}_k(1) - \tilde{\phi}_k(0) = \phi_k(1) - \phi_k(0)$ , but the particular form of (23) gives

$$\phi_k^{(r)}(s) = \sum_{l_1=1}^d \dots \sum_{l_r=1}^d \left[ \partial_{l_1} \dots \partial_{l_r} (F^{-1} - I)(\bar{x}_k + s(x - \bar{x}_k)) \prod_{i=1}^r (x - \bar{x}_k)_{l_i} \right], \quad (25)$$

so that  $\Phi_{k,(r)}$  is a polynomial mapping which coefficients involve evaluations of space derivatives of  $F^{-1}$  at  $\bar{x}_k$ . Also, (25) allows to specify the accuracy of the Taylor expansions (24) as follows: for all  $r \geq 1$  and every  $x$  in a localized domain  $\omega \subset B_\infty(\bar{x}_k, h\rho_\omega)$  with  $\rho_\omega > 0$ , we have

$$\|\Phi_{k,(r)}(x) - (F^{-1}(x) - x_k)\|_\infty = \left\| \int_0^1 \frac{(1-s)^r}{r!} \phi_k^{(r+1)}(s) ds \right\|_\infty \leq h^{r+1} \frac{(\rho_\omega)^{r+1}}{(r+1)!} |F^{-1}|_{r+1, \langle \omega \rangle} \quad (26)$$

where  $\langle \omega \rangle$  denotes the convex hull of  $\omega$ .

Thus, for  $r = 1$  we find  $\Phi_{k,(r)}(x) = J_{F^{-1}}(\bar{x}_k)(x - \bar{x}_k)$  where  $J_{F^{-1}}(\bar{x}_k) = J_F(x_k)^{-1}$  is the invertible Jacobian matrix of the backward flow. In particular,  $\Phi_{k,(r)}$  is invertible and the resulting linearly-transformed particles given by

$$T_{(1)}\varphi_{h,k}(x) := \varphi_h(\Phi_{k,(1)}(x)) = \varphi_h(J_k(x - \bar{x}_k)) \quad \text{with } \bar{x}_k = F(x_k), \quad J_k = J_{F^{-1}}(\bar{x}_k) = J_F(x_k)^{-1} \quad (27)$$

have a localized parallelogram support,

$$\text{supp}(T_{(1)}\varphi_{h,k}) = \bar{x}_k + J_k^{-1}(B_\infty(0, hc_p)) \subset B_\infty(\bar{\rho}_{h,k}, hc_p \|J_k^{-1}\|_\infty),$$

i.e., (18) now holds with  $\bar{\rho}_{h,k} := c_p \|J_{h,k}^{-1}\|_\infty \leq \bar{\rho} = c_p |F|_1$ . It follows that the above analysis applies readily to  $T_{(1)}$ , the only noticeable change being that instead of (21) we now write

$$\begin{aligned} \|e_{h,k}\|_{L^\infty} &= \sup_{x \in \bar{B}_{h,k}^e} |\varphi_h(\Phi_{k,(1)}(x)) - \varphi_h(F^{-1}(x) - F^{-1}(\bar{x}_k))| \\ &\leq |\varphi_h|_1 \sup_{x \in \bar{B}_{h,k}^e} \|\Phi_{k,(1)}(x) - (F^{-1}(x) - x_k)\|_\infty \\ &\leq h^{-(d-1)} \frac{1}{2} (\bar{\rho}_{h,k}^e)^2 |\varphi|_1 |F^{-1}|_{2, \bar{B}_{h,k}^e} \end{aligned} \quad (28)$$

with  $\bar{\rho}_{h,k}^e = c_p \max(\|J_k^{-1}\|_\infty, |F|_{1, \Sigma_{h,k}}) = c_p |F|_{1, \Sigma_{h,k}}$ , leading to

$$\|(T_{\text{ex}} - T_{(1)})f_h^0\|_{L^\infty} \leq hC\Theta_e(\bar{\rho}^e)^2 |F^{-1}|_2 \|f^{\text{in}}\|_{L^\infty} \quad (29)$$

with  $\bar{\rho}^e = c_p |F|_1 = \sup_{k \in \mathbb{Z}^d} \bar{\rho}_{h,k}^e$ ,  $\Theta_e = (2c_p)^d (1 + |F^{-1}|_1^d |F|_1^d)$ , and where as above,  $C$  depends only on  $d, p$ .

For larger values of  $r$ , care must be taken when defining  $T_{(r)}$ . Indeed, as  $\Phi_{k,(r)}$  may not be invertible, there is no guarantee that  $\|x - \bar{x}_k\|_\infty \lesssim h$  in the support of  $\varphi_j(\Phi_{k,(r)})$ . To overcome this difficulty we can define the transported particle as a restriction of the latter to a domain  $\bar{\Sigma}_{h,k}^\lambda$  that is *a priori* close to  $F(\Sigma_{h,k})$ , namely

$$T_{(r)}\varphi_{h,k}(x) = \varphi_h(\Phi_{k,(r)}(x)) \chi_{\bar{\Sigma}_{h,k}^\lambda}(x), \quad (30)$$

where again  $\Phi_{k,(r)}$  is the polynomial mapping defined by Equations (24)-(25),  $\chi$  denotes the set characteristic function, and where we have set

$$\bar{\Sigma}_{h,k}^\lambda := (\Phi_{k,(1)})^{-1}(B_\infty(0, hc_p(1 + \lambda))) = \bar{x}_k + J_k^{-1}(B_\infty(0, hc_p(1 + \lambda))). \quad (31)$$

Here  $\lambda$  is a free (and possibly local) parameter to be set in such a way that  $F(\Sigma_{h,k}) = \text{supp}(T_{\text{ex}}\varphi_{h,k})$  is contained in  $\bar{\Sigma}_{h,k}^\lambda$ , which will allow us to restrict the particle error term to the latter domain, and carry on the error estimates as in (28). In the remaining part of this section it will be convenient to let

$$\bar{\rho}_{h,k}(\lambda) := c_p(1 + \lambda)|F|_{1, \Sigma_{h,k}} \quad \text{and} \quad \bar{B}_{h,k}(\lambda) := B_\infty(\bar{x}_k, h\bar{\rho}_{h,k}(\lambda)).$$

Indeed we can check that  $T_{(r)}$  satisfies (18) with  $\bar{\rho}_{h,k} = \bar{\rho}_{h,k}(\lambda)$ , hence the corresponding particle transport errors  $e_{h,k} := (T_{(r)} - T_{\text{ex}})\varphi_{h,k}$  satisfy a bounded overlapping property similar to (19) with  $\Theta_e = (2c_p)^d (1 + (1 + \lambda)^d |F|_1^d |F^{-1}|_1^d)$ . Moreover, we infer from (20) that

$$\text{supp}(e_{h,k}) \subset (\text{supp}(T_{(r)}\varphi_{h,k}) \cup \text{supp}(T_{\text{ex}}\varphi_{h,k})) \subset (F(\Sigma_{h,k}) \cup \bar{\Sigma}_{h,k}^\lambda) \subset (\bar{B}_{h,k}(0) \cup \bar{B}_{h,k}(\lambda)) = \bar{B}_{h,k}(\lambda).$$

Our estimate for the error amplitude is given by the following Lemma.

**Lemma 3.1.** *Given  $h > 0$  and  $k \in \mathbb{Z}^d$ , the domains introduced in (20), (31) satisfy*

$$F(\Sigma_{h,k}) \subset \bar{\Sigma}_{h,k}^\lambda \quad \text{provided that} \quad \lambda \geq \lambda_{h,k}^{\min} := \frac{1}{2} hc_p |F|_{1, \Sigma_{h,k}}^2 |F^{-1}|_{2, \bar{B}_{h,k}(0)}. \quad (32)$$

*In particular, the particle transport error  $\bar{e}_{h,k}$  has its support in  $\bar{\Sigma}_{h,k}^\lambda$ , and satisfies*

$$\|e_{h,k}\|_{L^\infty} \leq h^{r-d} |\varphi|_1 \frac{(\bar{\rho}_{h,k}(\lambda))^{r+1}}{(r+1)!} |F^{-1}|_{r+1, \bar{B}_{h,k}(\lambda)}. \quad (33)$$

*Proof.* Based on the above discussion, for any  $y \in \Sigma_{h,k}$  we know that  $x := F(y)$  is in  $\bar{B}_{h,k}(0)$ . Hence using (26) we write

$$\begin{aligned} \|\Phi_{k,(1)}(x)\|_\infty &\leq \|y - x_k\|_\infty + \|\Phi_{k,(1)}(x) - (F^{-1}(x) - x_k)\|_\infty \\ &\leq hc_p + \frac{1}{2}h^2(\bar{\rho}_{h,k}(0))^2|F^{-1}|_{2,\bar{B}_{h,k}(0)} \\ &\leq hc_p(1 + \lambda), \end{aligned}$$

which shows (32). Turning to the error estimate, we then have

$$\begin{aligned} \|e_{h,k}\|_{L^\infty} &= \sup_{x \in \bar{\Sigma}_{h,k}^\lambda} |e_{h,k}(x)| \\ &\leq \sup_{x \in \bar{\Sigma}_{h,k}^\lambda} |\varphi_j(\Phi_{k,(r)}(x)) - \varphi_j(F^{-1}(x) - x_k)| \\ &\leq |\varphi_h|_1 \sup_{x \in \bar{B}_{h,k}(\lambda)} \|\Phi_{k,(r)}(x) - (F^{-1}(x) - x_k)\|_\infty \\ &\leq h^{r-d} |\varphi|_1 \frac{(\bar{\rho}_{h,k}(\lambda))^{r+1}}{(r+1)!} |F^{-1}|_{r+1, \bar{B}_{h,k}(\lambda)}, \end{aligned} \tag{34}$$

which completes the proof.  $\square$

A global estimate is then easily derived from the above results.

**Theorem 3.1.** *As above we consider B-spline particles  $\varphi_{h,k}$  of degree  $p$ , initially centered on the regular nodes  $x_k = kh$ ,  $k \in \mathbb{Z}^d$  and supported on the cubes  $\Sigma_{h,k} = B_\infty(x_k, hc_p)$  with  $c_p = \frac{p+1}{2}$ , see (10)-(11), and we denote by  $F = F_{0,\tau}$  the exact characteristic flow associated with Equation (1) on the time domain  $[0, \tau]$ . We let  $T_{(r)}$  be the  $r$ -th order particle transport operator defined by (27) for  $r = 1$ , or by (30)-(31) for  $r \geq 2$ . In the latter case we consider for simplicity a uniform localization parameter  $\lambda \geq \frac{1}{2}hc_p|F|_1^2|F^{-1}|_2$  and if  $r = 1$  we take  $\lambda = 0$ . Then the transported particles are localized by (18) with  $\bar{\rho}_{h,k}(\lambda) = c_p(1 + \lambda)|F|_{1,\Sigma_{h,k}}$ , and in particular they satisfy a uniformly bounded overlapping property*

$$\sup_{x \in \mathbb{R}^d} \#\{k \in \mathbb{Z}^d : T_{(r)}\varphi_{h,k}(x) \neq 0\} \leq ((p+1)(1+\lambda)|F|_1|F^{-1}|_1)^d.$$

Moreover, for any particle approximation  $f_h^0$  for which (15) holds, the global transport error satisfies

$$\|(T_{(r)} - T_{\text{ex}})f_h^0\|_{L^\infty} \leq Ch^r \Theta_e \frac{(c_p(1+\lambda)|F|_1)^{r+1}}{(r+1)!} |F^{-1}|_{r+1} \|f^{\text{in}}\|_{L^\infty}$$

with  $\Theta_e = (2c_p)^d(1 + (1+\lambda)^d|F|_1^d|F^{-1}|_1^d)$  and a constant  $C$  that only depends on  $d, p$ .

**Remark 3.2** (heterogeneous ‘‘particle’’ approximations). *As previously pointed out, our arguments do not rely on a smoothing kernel unlike classical analysis of particle methods [3], [25], and it is a simple exercise to extend the estimates stated in Theorem 3.1 to the heterogenous case where the ‘‘particles’’  $\varphi_{h,k}$  are not derived from a reference  $\varphi$  but instead are defined as piecewise polynomials with global continuity constraints (e.g., standard finite element bases) on unstructured meshes of  $\mathbb{R}^d$ , under the usual shape regularity and quasi-uniformity assumptions.*

### 3.3 A finite difference implementation of the LTP method

We now describe and analyze a finite difference implementation of the particle transport operator  $T_{(1)}$ , that will only make use of the numerical flow

$$F^n \approx F_{\text{ex}}^n := F_{t^n, t^{n+1}} \tag{35}$$

given by some explicit solver for the ODE (2) over the time step  $[t^n, t^{n+1}]$ . Specifically, we consider the following approximations. First, the exact transport operator

$$T_{\text{ex}}^n = T_{\text{ex}}[F_{\text{ex}}^n] : \varphi_{h,k}^n \mapsto \varphi_{h,k}^n \circ (F_{\text{ex}}^n)^{-1}, \tag{36}$$

when applied to a linearly transformed particle  $\varphi_{h,k}^n = \varphi_h(D_k^n(\cdot - x_k^n))$  as in (9), is approached by the first-order operator (27) defined in the previous section, namely

$$T_{(1)}[F_{\text{ex}}^n] : \varphi_{h,k}^n \mapsto \varphi_h(D_k^n J_{k,\text{ex}}^n(\cdot - F_{\text{ex}}^n(x_k^n))) \quad \text{with} \quad J_{k,\text{ex}}^n = (J_{F_{\text{ex}}^n}(x_k^n))^{-1}.$$

The Jacobian matrices involved in the latter are then approached by a finite difference scheme, and finally the values of  $F_{\text{ex}}^n$  are replaced by those of the numerical flow  $F^n$ . Thus, we set

$$T_h^n = T_h^n[F^n] : \varphi_{h,k}^n \mapsto \varphi_{h,k}^{n+1} = \varphi_h(D_k^{n+1}(\cdot - x_k^{n+1})) \quad (37)$$

with  $x_k^{n+1} := F^n(x_k^n)$  and  $D_k^{n+1} := D_k^n J_k^n$ . Here  $J_k^n \approx (J_{F_{\text{ex}}^n}(x_k^n))^{-1}$  is a numerical approximation of the backward Jacobian matrix obtained by first approximating the forward Jacobian by a centered finite difference scheme,

$$(\tilde{J}_k^n)_{i,j} := (2h)^{-1}((F^n)_i(x_k^n + he_j) - (F^n)_i(x_k^n - he_j)) \approx \partial_j(F_{\text{ex}}^n)_i(x_k^n), \quad i, j = 1, \dots, d, \quad (38)$$

and then letting

$$J_k^n := \det(\tilde{J}_k^n)^{\frac{1}{d}} (\tilde{J}_k^n)^{-1} \quad \text{or simply} \quad J_k^n := (\tilde{J}_k^n)^{-1}, \quad (39)$$

whether one desires a conservative transport operator (i.e., such that  $\int T_h^n \varphi_{h,k}^n = \int \varphi_{h,k}^n$ ), or not.

Note that  $\det(J_{F_{\text{ex}}^n}) = 1$  on  $\mathbb{R}^d$ , therefore it is reasonable to assume that the  $d \times d$  matrix  $\tilde{J}_k^n$  is invertible. In the following Lemma we establish a sufficient condition for this, together with some a priori estimates for the resulting approximations.

**Lemma 3.3.** *Let  $e_{\Delta t}^n := \|F^n - F_{\text{ex}}^n\|_{L^\infty}$  denote the error associated with the ODE solver. We have*

$$\det(\tilde{J}_k^n) \geq \theta_k^n := 1 - dh(\mu_{1,k}^n)^{d-1} \mu_{2,k}^n \quad (40)$$

with  $\mu_{1,k}^n := |F_{\text{ex}}^n|_{1, B_{h,k}^n} + dh^{-1}e_{\Delta t}^n$ ,  $\mu_{2,k}^n := \frac{1}{2}|F_{\text{ex}}^n|_{2, B_{h,k}^n} + dh^{-2}e_{\Delta t}^n$  and  $B_{h,k}^n := B_\infty(x_k^n, h)$ . Moreover, the approximated Jacobian matrix  $\tilde{J}_k^n$  satisfies

$$\|J_k^n - J_{(F_{\text{ex}}^n)^{-1}}(F_{\text{ex}}^n(x_k^n))\|_\infty \leq hd^2(\theta_k^n)^{-2}(\mu_{1,k}^n)^{2(d-1)}\mu_{2,k}^n \quad (41)$$

and

$$\|(J_k^n)^{-1} - (J_{(F_{\text{ex}}^n)^{-1}}(F_{\text{ex}}^n(x_k^n)))^{-1}\|_\infty \leq h(1 + (\theta_k^n)^{-\frac{d+1}{d}}(\mu_{1,k}^n)^d)\mu_{2,k}^n \quad (42)$$

provided  $\theta_k^n > 0$ . In particular, for all  $x \in \omega \subset B_\infty(x_k^{n+1}, h\rho_\omega)$  with  $\rho_\omega > 0$ , we have

$$\|J_k^n(x - x_k^{n+1}) - ((F_{\text{ex}}^n)^{-1}(x) - x_k^n)\|_\infty \leq h^2\rho_\omega(d^2(\theta_k^n)^{-2}(\mu_{1,k}^n)^{2(d-1)}\mu_{2,k}^n + \rho_\omega|(F_{\text{ex}}^n)^{-1}|_{2, \langle \omega \rangle})$$

where again,  $\langle \omega \rangle$  is the convex hull of  $\omega$ .

*Proof.* For conciseness, we drop the superscripts  $n$  and denote  $J_k^{\text{ex}} := J_{(F_{\text{ex}})^{-1}}(F(x_k))$ ,  $\tilde{J}_k^{\text{ex}} := (J_k^{\text{ex}})^{-1} = J_{F_{\text{ex}}}(x_k)$  and let  $\tilde{J}_k' \approx \tilde{J}_k^{\text{ex}}$  be the finite difference approximation obtained by substituting  $F$  by  $F_{\text{ex}}$  in (38), so that  $\|\tilde{J}_k' - \tilde{J}_k\|_\infty \leq h^{-1}de_{\Delta t}$ . We first observe that by construction, and with our particular choice of norms, we have

$$\|\tilde{J}_k^{\text{ex}}\|_\infty, \|\tilde{J}_k'\|_\infty \leq |F_{\text{ex}}|_{1, B_{h,k}} \quad \text{and} \quad \|\tilde{J}_k\|_\infty \leq \|\tilde{J}_k'\|_\infty + \|\tilde{J}_k - \tilde{J}_k'\|_\infty \leq \underbrace{|F_{\text{ex}}|_{1, B_{h,k}} + h^{-1}de_{\Delta t}}_{= \mu_{1,k}} \quad (43)$$

Next we write two Taylor formulas for  $s \mapsto F_{\text{ex}}(x_k + se_l)$  with  $l = 1, \dots, d$ , namely

$$F_{\text{ex}}(x_k + \sigma he_l) = F_{\text{ex}}(x_k) + \sigma h \partial_l F_{\text{ex}}(x_k) + \int_0^{\sigma h} (\sigma h - s) \partial_l^2 F_{\text{ex}}(x_k + se_l) ds, \quad \sigma = \pm 1,$$

which lead to

$$(2h)^{-1}[F_{\text{ex}}]_{x_k - he_l}^{x_k + he_l} = \partial_l F_{\text{ex}}(x_k) + (2h)^{-1} \int_0^h (h - s) (\partial_l^2 F_{\text{ex}}(x_k + se_l) - \partial_l^2 F_{\text{ex}}(x_k - se_l)) ds,$$

hence the finite difference approximations of  $\tilde{J}_k^{\text{ex}}$  satisfy

$$\|\tilde{J}_k' - \tilde{J}_k^{\text{ex}}\|_\infty \leq \frac{1}{2}h|F_{\text{ex}}|_{2, B_{h,k}} \quad \text{and} \quad \|\tilde{J}_k - \tilde{J}_k^{\text{ex}}\|_\infty \leq h \underbrace{(\frac{1}{2}|F_{\text{ex}}|_{2, B_{h,k}} + h^{-2}de_{\Delta t})}_{= \mu_{2,k}} \quad (44)$$

(note that one could gain one order in the estimate here, but we will not need it for the convergence order). We then derive from the multilinearity of the determinant that

$$|\det(\tilde{J}_k) - 1| = |\det(\tilde{J}_k) - \det(\tilde{J}_k^{\text{ex}})| \leq d \|\tilde{J}_k - \tilde{J}_k^{\text{ex}}\|_\infty \max(\|\tilde{J}_k\|_\infty, \|\tilde{J}_k^{\text{ex}}\|_\infty)^{d-1} \leq hd\mu_{2,k}(\mu_{1,k})^{d-1} \quad (45)$$

which shows (40). Next if  $\theta_k > 0$ , by using the cofactors formula for the inverse matrices we find that

$$\|J_k^{\text{ex}}\|_\infty \leq d \frac{\|\tilde{J}_k^{\text{ex}}\|_\infty^{d-1}}{\det(\tilde{J}_k^{\text{ex}})} \leq d |F_{\text{ex}}|_{1, B_{h,k}}^{d-1} \leq d(\mu_{1,k})^{d-1} \quad \text{and} \quad \|\tilde{J}_k^{-1}\|_\infty \leq d \frac{\|\tilde{J}_k\|_\infty^{d-1}}{\det(\tilde{J}_k)} \leq d\theta_k^{-1}(\mu_{1,k})^{d-1}$$

hence the non-conservative approximated Jacobian  $J_k := \tilde{J}_k^{-1}$  satisfies

$$\|J_k - J_k^{\text{ex}}\|_\infty \leq \|J_k^{\text{ex}}\|_\infty \|\tilde{J}_k - \tilde{J}_k^{\text{ex}}\|_\infty \|J_k\|_\infty \leq hd^2\theta_k^{-1}(\mu_{1,k})^{2(d-1)}\mu_{2,k}.$$

Turning to the conservative case, we next infer from  $\theta_k \leq \min\{1, \det(\tilde{J}_k)\}$  that

$$|1 - \det(\tilde{J}_k)^\alpha| = \left| \int_1^{\det(\tilde{J}_k)} \alpha z^{\alpha-1} dz \right| \leq |\alpha|(\theta_k)^{\alpha-1} |1 - \det(\tilde{J}_k)|, \quad \text{for } \alpha \leq 1. \quad (46)$$

Using (46) with  $\alpha = \frac{1}{d}$ , we then obtain

$$\begin{aligned} \|J_k - J_k^{\text{ex}}\| &= \|\det(\tilde{J}_k)^{\frac{1}{d}}(\tilde{J}_k)^{-1} - (\tilde{J}_k^{\text{ex}})^{-1}\| \leq |\det(\tilde{J}_k)^{\frac{1}{d}} - 1| \|(\tilde{J}_k)^{-1}\| + \|(\tilde{J}_k)^{-1}\| \|\tilde{J}_k - \tilde{J}_k^{\text{ex}}\| \|J_k^{\text{ex}}\| \\ &\leq hd^2\theta_k^{-2}(\mu_{1,k})^{2(d-1)}\mu_{2,k} \end{aligned}$$

which proves (41). Next we note that (44) gives  $\|J_k^{-1} - (J_k^{\text{ex}})^{-1}\|_\infty \leq h\mu_{2,k}$  in the non-conservative case, while in the conservative case we write

$$\begin{aligned} \|J_k^{-1} - (J_k^{\text{ex}})^{-1}\|_\infty &= \|\det(\tilde{J}_k)^{-\frac{1}{d}}\tilde{J}_k - \tilde{J}_k^{\text{ex}}\|_\infty \leq |\det(\tilde{J}_k)^{-\frac{1}{d}} - 1| \|\tilde{J}_k\|_\infty + \|\tilde{J}_k - \tilde{J}_k^{\text{ex}}\|_\infty \\ &\leq h(1 + (\theta_k)^{-\frac{1}{d}-1}\mu_{1,k}^d)\mu_{2,k} \end{aligned}$$

where we have used (46) with  $\alpha = -\frac{1}{d}$ , together with (45), (43). This shows that (42) is valid in both cases. We finally invoke (26) with  $r = 1$  to complete the proof.  $\square$

### 3.4 Intermission: localization of particles with deformed shape

For practical purposes, such as the computation of pointwise density values  $f_h^n(x) = \sum_k w_k \varphi_k^n(x)$ , it is important to access in a reasonable amount of time the particles which support contain any given  $x \in \mathbb{R}^d$ . This can be done with a localization pre-processing that subdivides the phase space into simple domains such as dyadic cells  $\Omega_m = 2^{-j}(\prod_{i=1}^d [m_i, m_i + 1])$ ,  $m \in \mathbb{Z}^d$ , with  $2^{-j} \approx h$ , and then writes in the scope of every such cell the indices of the overlapping particles, namely

$$K_m^n = \{k \in \mathbb{Z}^d : \varphi_{h,k}^n(\Omega_m) \neq 0\}, \quad m \in \mathbb{Z}^d. \quad (47)$$

In practice, one can run a cell marking algorithm for each newly transported particle  $\varphi_{j,k}^n$ , starting with the (left) cell  $\Omega_m$  containing  $x_k^n$ , i.e.  $m = \lfloor 2^j x_k^n \rfloor$ , and recursively testing the adjacent cells to see whether they overlap the parallelogram support of  $\varphi_{h,k}^n$ . To perform this test we can use the following result with  $A = (D_k^n)^{-1}$ ,  $B = B_\infty(0, hc_p)$  and  $B' = B_\infty(2^{-j}(m + \frac{1}{2}) - x_k^n, 2^{-j-1})$ .

**Lemma 3.4.** *Let  $B = \prod_{i=1}^d [x_i - r_i, x_i + r_i]$  and  $B' = \prod_{i=1}^d [x'_i - r'_i, x'_i + r'_i]$  be two orthotopes aligned with the coordinate axes, and  $A$  an invertible  $d \times d$  matrix. We have*

$$AB \cap B' \neq \emptyset \iff |(Ax - x')_i| \leq \tilde{r}_i + r'_i \quad \text{and} \quad |(x - A^{-1}x')_i| \leq r_i + \tilde{r}'_i \quad \text{for } i = 1 \dots d$$

with  $\tilde{r}_i := \sum_{j=1}^d |A_{i,j}|r_j$  and  $\tilde{r}'_i := \sum_{j=1}^d |A_{i,j}^{-1}|r'_j$ .

*Proof.* Observe that  $\tilde{B} := \prod_{i=1}^d [(Ax)_i - \tilde{r}_i, (Ax)_i + \tilde{r}_i]$  and  $\tilde{B}' := \prod_{i=1}^d [(A^{-1}x)_i - \tilde{r}'_i, (A^{-1}x)_i + \tilde{r}'_i]$  are the smallest orthotopes aligned with the coordinate axes that contain  $AB$  and  $A^{-1}B'$ , respectively. Since the above two sets of inequalities hold iff  $\tilde{B}$  and  $B$  intersect  $B'$  and  $\tilde{B}'$  respectively, the  $\Rightarrow$  direction is easily checked. In order to prove the  $\Leftarrow$  direction we make use of the fact that two disjoint convex polytopes can always be separated by the hyperplane supported by one  $d-1$  dimensional face of one polytope. Thus, if  $AB$  and  $B'$  are disjoint, we can choose a face of  $B'$  or a face of  $AB$ . This respectively implies that  $\tilde{B} \cap B' = \emptyset$  or  $B \cap \tilde{B}' = \emptyset$ , and hence ends the proof.  $\square$

### 3.5 A priori estimates for a fully discrete LTP scheme

In this section we establish a priori estimates for the fully discrete particle scheme consisting of an initialization step using the B-spline quasi-interpolation (12), and of a series of transport steps using the LTP transport operator (37)-(39), and no remappings. Thus, we consider

$$f_h^0 := A_h f^{\text{in}} \quad \text{and} \quad f_h^{n+1} := T_h^n f_h^n \quad \text{for } n = 0, \dots, N-1, \quad (48)$$

with  $\Delta t = \tau/N$ .  $L^\infty$  convergence of this scheme will be established in Theorem 3.2, together with uniform bounds for the particle overlapping. A local (single particle) error estimate will be shown as well, that will be of practical use in the adaptive multilevel LTP scheme described in Section 4.

To express our estimates in terms of the smoothness of the velocity field  $u$ , we begin with local bounds for the characteristic flow.

**Lemma 3.5.** *Given a domain  $\omega \subset \mathbb{R}^d$ , an integer  $m$  and two instants  $s, t \in [0, \tau]$ , we denote*

$$|u|_{m,(s,t,\omega)} := \sup_{t' \in [s,t]} |u(t', \cdot)|_{m, F_{s,t'}(\omega)} = \sup_{t' \in [s,t]} \max_{i=1, \dots, d} \left\{ \sum_{l_1=1}^d \cdots \sum_{l_m=1}^d \sup_{x \in \omega} |\partial_{l_1} \cdots \partial_{l_m} u_i(t', F_{s,t'}(x))| \right\}$$

where  $F_{s,t'}$  is the flow of  $u$  between  $s$  and  $t'$ , as above. Then we have

$$|F_{s,t} - I|_{1,\omega} \leq c_{1,u} \exp(c_{1,u}) \quad \text{and} \quad |F_{s,t}|_{2,\omega} \leq c_{2,u} \exp(c_{1,u})(1 + c_{1,u} \exp(c_{1,u})) \quad (49)$$

with  $c_{m,u} = |t-s| |u|_{m,(s,t,\omega)}$ ,  $m = 1, 2$ .

*Proof.* Rewriting (2) as  $\partial_t F_{s,t}(x) = u(t, F_{s,t}(x))$ , we obtain that for  $i, l = 1, \dots, d$ ,

$$\begin{aligned} \partial_t \partial_l (F_{s,t} - I)_i(x) &= \partial_l \partial_t (F_{s,t})_i(x) \\ &= \sum_{l'=1}^d \partial_{l'} u_i(t, F_{s,t}(x)) \partial_l (F_{s,t})_{l'}(x) \\ &= \sum_{l'=1}^d \partial_{l'} u_i(t, F_{s,t}(x)) \partial_l (F_{s,t} - I)_{l'}(x) + \partial_l u_i(t, F_{s,t}(x)). \end{aligned}$$

In particular, using  $F_{s,s} = I$  we find

$$\partial_l (F_{s,t} - I)_i(x) = \int_s^t \left[ \sum_{l'=1}^d \partial_{l'} u_i(t', F_{s,t'}(x)) \partial_l (F_{s,t'} - I)_{l'}(x) + \partial_l u_i(t', F_{s,t'}(x)) \right] dt',$$

so that taking the supremum over  $x \in \omega$ , summing over  $l = 1, \dots, d$  and taking the maximum over  $i = 1, \dots, d$  yields

$$\begin{aligned} |F_{s,t} - I|_{1,\omega} &\leq |u|_{1,(s,t,\omega)} (|t-s| + \int_s^t |F_{s,t'} - I|_{1,\omega} dt') \\ &\leq |t-s| |u|_{1,(s,t,\omega)} \exp(|t-s| |u|_{1,(s,t,\omega)}) \end{aligned}$$

where the second inequality follows from the Gronwall Lemma in integral form [4]. This shows the first part of (49). In particular, using  $|I|_{1,\omega} = 1$  this shows that

$$|F_{s,t}|_{1,\omega} \leq 1 + |t-s| |u|_{1,(s,t,\omega)} \exp(|t-s| |u|_{1,(s,t,\omega)}). \quad (50)$$

Turning to the second derivatives, using again  $F_{s,s} = I$  we write

$$\begin{aligned} \partial_{l_1} \partial_{l_2} (F_{s,t})_i(x) &= \int_s^t \left[ \sum_{l'_1=1}^d \sum_{l'_2=1}^d \partial_{l'_1} \partial_{l'_2} u_i(t', F_{s,t'}(x)) \partial_{l_1} (F_{s,t'})_{l'_1}(x) \partial_{l_2} (F_{s,t'})_{l'_2}(x) \right. \\ &\quad \left. + \sum_{l'=1}^d \partial_{l'} u_i(t', F_{s,t'}(x)) \partial_{l_1} \partial_{l_2} (F_{s,t'})_{l'}(x) \right] dt' \end{aligned}$$

so that taking the supremum over  $x \in \omega$ , summing over  $l_1, l_2 = 1, \dots, d$  and taking the maximum over  $i = 1, \dots, d$  now gives

$$\begin{aligned} |F_{s,t}|_{2,\omega} &\leq |u|_{2,(s,t,\omega)} \int_s^t |F_{s,t'}|_{1,\omega}^2 dt' + |u|_{1,(s,t,\omega)} \int_s^t |F_{s,t'}|_{2,\omega} dt' \\ &\leq |u|_{2,(s,t,\omega)} \left( \int_s^t |F_{s,t'}|_{1,\omega}^2 dt' \right) \exp(|t-s||u|_{1,(s,t,\omega)}) \\ &\leq |t-s||u|_{2,(s,t,\omega)} \left( 1 + |t-s||u|_{1,(s,t,\omega)} \exp(|t-s||u|_{1,(s,t,\omega)}) \right)^2 \exp(|t-s||u|_{1,(s,t,\omega)}) \end{aligned}$$

where we have used again the Gronwall Lemma, and (50). This shows the second part of (49).  $\square$

**Corollary 3.6.** *Let  $\nu_{1,\omega}^n := |u|_{1,\xi} \exp(\Delta t |u|_{1,\xi})$  and  $\nu_{2,\omega}^n := |u|_{2,\xi} \exp(\Delta t |u|_{1,\xi})(1 + \Delta t \nu_{1,\omega}^n)$  with  $\xi = (t^n, t^{n+1}, \omega)$ . Then we have*

$$|(F_{\text{ex}}^n)^{-1}|_{1, F_{\text{ex}}^n(\omega)} = |F_{\text{ex}}^n|_{1,\omega} \leq 1 + \Delta t \nu_{1,\omega}^n \quad \text{and} \quad |(F_{\text{ex}}^n)^{-1}|_{2, F_{\text{ex}}^n(\omega)} = |F_{\text{ex}}^n|_{2,\omega} \leq \Delta t \nu_{2,\omega}^n. \quad (51)$$

In particular, denoting  $\nu_i^n := \nu_{i,\mathbb{R}^d}^n$  yields

$$|(F_{\text{ex}}^n)^{\pm 1}|_1 \leq 1 + \Delta t \nu_1^n \quad \text{and} \quad |(F_{\text{ex}}^n)^{\pm 1}|_2 \leq \Delta t \nu_2^n. \quad (52)$$

*Proof.* The first estimate is obtained with Lemma 3.5, observing that  $F_{t^{n+1},t}(F_{\text{ex}}^n(x)) = F_{t^n,t}(x)$ . The second one follows from the fact that  $F_{\text{ex}}^n$  is a diffeomorphism.  $\square$

**Assumption 3.7.** *In view of Corollary 3.6, one can expect to derive from Lemma 3.3 that the error resulting from the linearization of the flow around  $x_k^{n+1}$  behaves like*

$$\|J_k^n(x - x_k^{n+1}) - ((F_{\text{ex}}^n)^{-1}(x) - x_k^n)\| \lesssim \Delta t \|x - x_k^{n+1}\|^2 (1 + \Delta t \nu_1^n + h^{-1} e_{\Delta t}^n)^{2(d-1)} (\nu_2^n + \frac{h^{-2} e_{\Delta t}^n}{\Delta t})$$

so that it seems natural to ask that  $h^{-2} e_{\Delta t}^n \sim \Delta t$ . Therefore we will assume in the sequel that  $h$  and  $\Delta t$  are such that

$$h^{-2} e_{\Delta t}^n \leq \alpha \Delta t, \quad (53)$$

where  $\alpha > 0$  is a fixed constant. Note that if an  $r$ -th order ODE solver is used to compute the numerical flow, the above condition reads  $\Delta t \leq C \alpha h^{\frac{2}{r}}$  with a constant  $C$  depending on the smoothness of  $u$ , typically through  $|u|_{r+1,(t^n, t^{n+1}, \mathbb{R}^d)}$ .

For the subsequent analysis it will be convenient to introduce the following measures of the velocity smoothness,

$$\begin{aligned} \kappa_{1,(h,k)}^n &:= \nu_{1, B_{h,k}^n}^n + h d \alpha, & \kappa_{3,(h,k)}^n &:= 2d(1 + \Delta t \kappa_{1,(h,k)}^n)^{d-1} \kappa_{2,(h,k)}^n, \\ \kappa_{2,(h,k)}^n &:= \frac{1}{2} \nu_{2, B_{h,k}^n}^n + d \alpha, & \kappa_{4,(h,k)}^n &:= d^2(1 + h \Delta t \kappa_{3,(h,k)}^n)^2 (1 + \Delta t \kappa_{1,(h,k)}^n)^{2(d-1)} \kappa_{2,(h,k)}^n \end{aligned} \quad (54)$$

and their global-in-space versions,

$$\begin{aligned} \kappa_{1,h}^n &:= \nu_1^n + h d \alpha, & \kappa_{3,h}^n &:= 2d(1 + \Delta t \kappa_{1,h}^n)^{d-1} \kappa_{2,h}^n, \\ \kappa_{2,h}^n &:= \frac{1}{2} \nu_2^n + d \alpha, & \kappa_{4,h}^n &:= d^2(1 + h \Delta t \kappa_{3,h}^n)^2 (1 + \Delta t \kappa_{1,h}^n)^{2(d-1)} \kappa_{2,h}^n, \end{aligned} \quad (55)$$

and finally their global-in-time counterparts  $\kappa_{i,h}$ ,  $i = 1, \dots, 4$ , defined using

$$\nu_1 = |u|_{1,\xi} \exp(\Delta t |u|_{1,\xi}) \quad \text{and} \quad \nu_2 := |u|_{2,\xi} \exp(\Delta t |u|_{1,\xi})(1 + \Delta t \nu_1) \quad \text{with } \xi = (0, \tau, \mathbb{R}^d). \quad (56)$$

Equipped with the local measures (54), we now derive the following estimates from Lemma 3.3.

**Corollary 3.8.** *Provided  $h$  and  $\Delta t$  satisfy (53) and the additional mild condition*

$$h\Delta t\kappa_{3,(h,k)}^n \leq 1 \quad (57)$$

the finite-difference approximation (38) of the forward Jacobian yields an invertible matrix  $\tilde{J}_k^n$  satisfying

$$\det(\tilde{J}_k^n)^{-1} \leq (\theta_k^n)^{-1} \leq 1 + h\Delta t\kappa_{3,(h,k)}^n. \quad (58)$$

In particular, the operator  $T_h^n$  is well defined by (37)-(39). Moreover, given  $\omega \subset B_\infty(x_k^{n+1}, h\rho_\omega)$  with  $\rho_\omega > 0$ , the linearized flow based on the approximated backward Jacobian  $J_k^n$  satisfies

$$\sup_{x \in \omega} \|J_k^n(x - x_k^{n+1}) - ((F_{\text{ex}}^n)^{-1}(x) - x_k^n)\|_\infty \leq h^2(\Delta t\rho_\omega\kappa_{4,(h,k)}^n + (\rho_\omega)^2|(F_{\text{ex}}^n)^{-1}|_{2,\langle\omega\rangle}), \quad (59)$$

where  $\langle\omega\rangle$  is the convex hull of  $\omega$ .

*Proof.* According to (51), we have

$$\mu_{1,(h,k)}^n \leq 1 + \Delta t\kappa_{1,(h,k)}^n \quad \text{and} \quad \mu_{2,(h,k)}^n \leq \Delta t\kappa_{2,(h,k)}^n. \quad (60)$$

For  $h\Delta t\kappa_{3,(h,k)}^n \leq 1$ , we then infer from (40) that

$$\det(\tilde{J}_k^n) \geq \theta_k^n \geq 1 - hd(1 + \Delta t\kappa_{1,(h,k)}^n)^{d-1}\Delta t\kappa_{2,(h,k)}^n \geq 1 - \frac{1}{2}h\Delta t\kappa_{3,(h,k)}^n \geq \frac{1}{2}h\Delta t\kappa_{3,(h,k)}^n > 0.$$

This shows the invertibility of  $\tilde{J}_k^n$  and also gives (58), hence the first claim. Estimate (59) follows then from Lemma 3.3, without difficulty.  $\square$

We are now in position to state a priori estimates for the local (single particle) transport error, the particle overlapping and the global convergence of the fully discrete LTP scheme. Again, let us emphasize that although the following result is established for B-spline particles, the same arguments would easily apply to more general approximation settings such as continuous finite element basis functions, see Remark 3.2.

**Theorem 3.2.** *Let  $f$  be the solution of Equation (1), and  $h, \Delta t = \tau/N$  be such that conditions (57) and (53) hold with a fixed  $\alpha > 0$ . Then the numerical solutions computed by the scheme (48) satisfy*

$$\|f_h^n - f(t^n)\|_{L^\infty} \leq h(c_T\|f^{\text{in}}\|_{L^\infty} + c_A|f^{\text{in}}|_1) \quad \text{for } n = 0, \dots, N, \quad (61)$$

and with constants  $c_T, c_A$  independent of  $h$  and  $\Delta t$ . Moreover, the particles  $\varphi_{h,k}^n = \varphi_h(D_k^n(\cdot - x_k^n))$  composing  $f_h^n$  have uniformly bounded supports  $\Sigma_{h,k}^n := \text{supp}(\varphi_{h,k}^n)$  and overlapping constants. Specifically, we have

$$\Sigma_{h,k}^n \subset B_\infty(x_k^n, hc_p \exp(\tau(\frac{\kappa_{3,h}}{d} + \kappa_{1,h}))) \quad (62)$$

and

$$\sup_{x \in \mathbb{R}^d} \#\left(\{k \in \mathbb{Z}^d : x \in \Sigma_{h,k}^n\}\right) \leq \Theta_h := (2 \exp(\tau\nu_1)(c_p \exp(\tau(\frac{\kappa_{3,h}}{d} + \kappa_{1,h})) + h\tau\alpha))^d \quad (63)$$

for  $n = 0, \dots, N$ , with  $c_p = \frac{p+1}{2}$  and velocity smoothness measures  $\nu_i, \kappa_{i,h}$  defined in Corollary 3.6 and Equations (55)-(56). Finally, the single particle transport errors  $e_{h,k}^{n+1} := (T_h^n - T_{\text{ex}}^n)\varphi_{h,k}^n$  can be estimated by

$$\|e_{h,k}^{n+1}\|_{L^\infty} \leq h^{1-d}|\varphi|_1\|D_k^n\|_\infty(\Delta t\rho_{h,k}^{e,n+1}\kappa_{4,(h,k)}^n + (\rho_{h,k}^{e,n+1})^2|(F_{\text{ex}}^n)^{-1}|_{2,\langle\Sigma_{h,k}^{n+1} \cup F_{\text{ex}}^n(\Sigma_{h,k}^n)\rangle}) \quad (64)$$

with

$$\rho_{h,k}^{e,n+1} := h\alpha + c_p\|(D_k^n)^{-1}\|_\infty \max\left\{(1 + h\Delta t\kappa_{3,(h,k)}^n)^{\frac{1}{d}}(1 + \Delta t\kappa_{1,(h,k)}^n), 1 + \Delta t\nu_{1,\Sigma_{h,k}^n}^n\right\} \quad (65)$$

and local smoothness measures defined in Corollary 3.6 and Equation (54).

*Proof.* We first observe that the particles supports satisfy

$$\Sigma_{h,k}^n := \text{supp}(\varphi_{h,k}^n) = x_k^n + (D_k^n)^{-1}(B_\infty(0, hc_p)) \subset B_\infty(x_k^n, hc_p \| (D_k^n)^{-1} \|_\infty), \quad (66)$$

hence particles transported along the exact flow  $F_{\text{ex}}^n$  are supported on

$$\text{supp}(T_{\text{ex}}^n \varphi_{h,k}^n) = F_{\text{ex}}^n(\Sigma_{h,k}^n) \subset B_\infty(x_k^{n+1}, e_{\Delta t}^n + hc_p \| (D_k^n)^{-1} \|_\infty |F_{\text{ex}}^n|_{1, \Sigma_{h,k}^n}).$$

Turning to the single-particle transport errors  $e_{h,k}^{n+1} = (T_h^n - T_{\text{ex}}^n) \varphi_{h,k}^n = \varphi_{h,k}^{n+1} - T_{\text{ex}}^n \varphi_{h,k}^n$ , we next derive from (43), (60) that

$$\| \tilde{J}_k^n \|_\infty \leq 1 + \Delta t \kappa_{1,(h,k)}^n, \quad (67)$$

and using  $(J_k^n)^{-1} = \tilde{J}_k^n$  or (39), (58) in the conservative case, we write

$$\| (J_k^n)^{-1} \|_\infty \leq \max(1, \det(\tilde{J}_k^n)^{-\frac{1}{d}}) \| \tilde{J}_k^n \|_\infty \leq (1 + h \Delta t \kappa_{3,(h,k)}^n)^{\frac{1}{d}} (1 + \Delta t \kappa_{1,(h,k)}^n).$$

It then follows from  $D_k^{n+1} = D_k^n J_k^n$  that

$$\begin{aligned} \text{supp}(e_{h,k}^{n+1}) &\subset \Sigma_{h,k}^{n+1} \cup F_{\text{ex}}^n(\Sigma_{h,k}^n) \\ &\subset B_\infty(x_k^{n+1}, e_{\Delta t}^n + hc_p \| (D_k^n)^{-1} \|_\infty \max\{ \| (J_k^n)^{-1} \|_\infty, |F_{\text{ex}}^n|_{1, \Sigma_{h,k}^n} \}) \\ &\subset B_\infty(x_k^{n+1}, h \rho_{h,k}^{e,n+1}) \end{aligned} \quad (68)$$

with  $\rho_{h,k}^{e,n+1}$  defined as in (65). According to (59), this gives

$$\begin{aligned} \| e_{h,k}^{n+1} \|_{L^\infty} &= \sup_{x \in \Sigma_{h,k}^{n+1} \cup F_{\text{ex}}^n(\Sigma_{h,k}^n)} | \varphi_h(D_k^n J_k^n(x - x_k^{n+1})) - \varphi_h(D_k^n ((F_{\text{ex}}^n)^{-1}(x) - x_k^n)) | \\ &\leq | \varphi_h |_1 \| D_k^n \|_\infty \sup_{x \in \Sigma_{h,k}^{n+1} \cup F_{\text{ex}}^n(\Sigma_{h,k}^n)} \| J_k^n(x - x_k^{n+1}) - ((F_{\text{ex}}^n)^{-1}(x) - x_k^n) \|_\infty \\ &\leq h^{1-d} | \varphi |_1 \| D_k^n \|_\infty (\Delta t \rho_{h,k}^{e,n+1} \kappa_{4,(h,k)}^n + (\rho_{h,k}^{e,n+1})^2 | (F_{\text{ex}}^n)^{-1} |_{2, (\Sigma_{h,k}^{n+1} \cup F_{\text{ex}}^n(\Sigma_{h,k}^n))}) \end{aligned} \quad (69)$$

which is (64). To establish global estimates, we next let  $\Theta_{h,e}$  denote an upper bound for the overlapping constant of the transport errors, i.e.,

$$\max_{n \leq N} \sup_{x \in \mathbb{R}^d} \#(\{k \in \mathbb{Z}^d : e_{h,k}^n(x) \neq 0\}) \leq \Theta_{h,e}$$

and use the bound  $|w_k(f^{\text{in}})| \leq \|a\|_{\ell^1} \|f^{\text{in}}\|_{L^\infty}$  satisfied by the weights obtained with (12) to write

$$\begin{aligned} \| (T_h^n - T_{\text{ex}}^n) f_h^n \|_{L^\infty} &= \| \sum_{k \in \mathbb{Z}^d} w_k(f^{\text{in}}) e_{h,k}^{n+1} \|_{L^\infty} \leq \Theta_{h,e} \sup_{k \in \mathbb{Z}^d} \|w_k(f^{\text{in}}) e_{h,k}^{n+1}\|_{L^\infty} \\ &\leq h \Delta t \Theta_{h,e} | \varphi |_1 c_{h,e}^{n+1} (\kappa_{4,h}^n + c_{h,e}^{n+1} \nu_2^n) (\sup_{k \in \mathbb{Z}^d} \| D_k^n \|_\infty) \|a\|_{\ell^1} \|f^{\text{in}}\|_{L^\infty} \end{aligned} \quad (70)$$

with  $c_{h,e}^{n+1} := h\alpha + c_p (\sup_{k \in \mathbb{Z}^d} \| (D_k^n)^{-1} \|_\infty) (1 + h \Delta t \kappa_{3,h}^n)^{\frac{1}{d}} (1 + \Delta t \kappa_{1,h}^n)$ . We next observe that

$$\| (D_k^n)^{-1} \|_\infty \leq \prod_{m=0}^{n-1} | \theta_k^m |^{-\frac{1}{d}} \| \tilde{J}_k^m \|_\infty \leq (1 + \Delta t \kappa_{3,h}^n)^{\frac{n}{d}} (1 + \Delta t \kappa_{1,h}^n)^n \leq \exp(\tau(\frac{\kappa_{3,h}}{d} + \kappa_{1,h})) \quad (71)$$

holds for all  $n \leq N$  in both the conservative and the non-conservative cases, since  $\theta_k^m \leq 1$ . Using (66), this yields uniform bounds for the both the particles and the transport error supports: we indeed obtain (62) in the one hand, and in the other hand we can bound the localization constant in (68) with

$$c_{h,e}^{n+1} \leq h\alpha + c_p (1 + \Delta t \kappa_{3,h}^n)^{\frac{n+1}{d}} (1 + \Delta t \kappa_{1,h}^n)^{n+1} \leq h\alpha + c_p \exp(\tau(\frac{\kappa_{3,h}}{d} + \kappa_{1,h})) =: c_{h,e},$$

where we have used that  $\nu_1^n \leq \nu_1 \leq \kappa_{1,h}$ . We observe that (71) also allows to bound the overlapping of both the particles and the transport errors. Indeed, considering an arbitrary  $x^n \in \text{supp}(\varphi_{h,k}^n)$  and letting  $x^m := (F_{\text{ex}}^m)^{-1}(x^{m+1})$  for  $m = n-1, \dots, 0$ , we first derive from (52) that

$$\| x^m - x_k^m \|_\infty \leq | (F_{\text{ex}}^m)^{-1} |_1 \| x^{m+1} - F_{\text{ex}}^m(x_k^{m+1}) \|_\infty \leq (1 + \Delta t \nu_1) (\| x^{m+1} - x_k^{m+1} \|_\infty + e_{\Delta t}^m)$$

where  $e_{\Delta t}^m := \|F^m - F_{\text{ex}}^m\|_{L^\infty}$  is the ODE solver error introduced in Lemma 3.3. Using (53) and (71) we then write

$$\begin{aligned} \|x^0 - x_k\|_\infty &\leq (1 + \Delta t \nu_1)^n (\|x^n - x_k^n\|_\infty + nh^2 \Delta t \alpha) \\ &< h(1 + \Delta t \nu_1)^n (c_p \|(D_k^n)^{-1}\|_\infty + h\tau\alpha) \\ &< h \exp(\tau \nu_1) (c_p \exp(\tau(\frac{\kappa_{3,h}}{d} + \kappa_{1,h})) + h\tau\alpha). \end{aligned}$$

Since the initial particles are centered on the structured nodes  $x_k = hk$ ,  $k \in \mathbb{Z}^d$ , this shows that the number of overlapping particles is bounded uniformly with (63), and as for the errors terms we have

$$\Theta_{h,e} \leq 2\Theta_h,$$

given that the particle overlapping is not increased by the exact transport operator. To finally prove the global error estimate, we next derive from Corollary 3.8 that

$$\det(D_k^n) \leq \prod_{m=0}^{n-1} (\theta_k^m)^{-1} \leq (1 + \Delta t \kappa_{3,h})^n \leq \exp(\tau \kappa_{3,h})$$

in the nonconservative case, whereas  $\det(D_k^n) = 1$  by construction in the conservative case. Noting that (71) becomes  $\|(D_k^n)^{-1}\|_\infty \leq (1 + \Delta t \kappa_{1,h})^n$  in this latter case, and using the cofactor formula  $A^{-1} = \det(A)^{-1} C^t$  that involves the transposed cofactor matrix, with a little algebra we find in both cases that

$$\|D_k^n\|_\infty \leq d \det(D_k^n) \|(D_k^n)^{-1}\|_\infty^{d-1} \leq d \exp(\tau(\kappa_{3,h} + \kappa_{1,h}(d-1))). \quad (72)$$

Gathering the above estimates yields then an a priori estimate for the transport error (70),

$$\|(T_h^n - T_{\text{ex}}^n) f_h^n\|_{L^\infty} \leq c_{h,\tau} h \Delta t \|f^{\text{in}}\|_{L^\infty}$$

with

$$c_{h,\tau} := 2\Theta_h |\varphi|_1 c_{h,e} (\kappa_{4,h} + c_{h,e} \nu_2) d \exp(\tau(\kappa_{3,h} + \kappa_{1,h}(d-1))) \|a\|_{\ell^1}.$$

In particular, for the global error  $e_h^{n+1} := f_h^{n+1} - f^{(n+1)} = T_h^n f_h^n - T_{\text{ex}}^n f(t^n)$  we obtain

$$\begin{aligned} \|e_h^{n+1}\|_{L^\infty} &\leq \|(T_h^n - T_{\text{ex}}^n) f_h^n\|_{L^\infty} + \|T_{\text{ex}}^n e_h^n\|_{L^\infty} \\ &\leq \|(T_h^n - T_{\text{ex}}^n) f_h^n\|_{L^\infty} + \|e_h^n\|_{L^\infty} \\ &\leq \sum_{m=0}^n \|(T_h^m - T_{\text{ex}}^m) f_h^m\|_{L^\infty} + \|f_h^0 - f^{\text{in}}\|_{L^\infty} \\ &\leq h(\tau c_{h,\tau} \|f^{\text{in}}\|_{L^\infty} + c_A |f^{\text{in}}|_1) \end{aligned}$$

where we have used Estimate (14) with  $q = 1$ , i.e.  $c_A$  only depends on  $p$ ,  $d$  and  $\|\varphi\|_{L^\infty}$ . The final convergence result follows then by observing that  $c_{h,\tau}$  increases with  $h$ , and is bounded by a constant that only depends on  $h_{\text{max}}$ ,  $d$ ,  $\alpha$ ,  $\tau$  and on the velocity smoothness through  $u|_{i,(0,\tau,\mathbb{R}^d)}$ ,  $i = 1, 2$ .  $\square$

## 4 Adaptive transport with multilevel particles

To illustrate the flexibility of our approach, we now describe one adaptive version of the LTP scheme. Here the goal is to save computational time where low resolution approximations do not deteriorate the global accuracy of the simulations, and to implement that principle we use a hierarchy of particles with dyadic scales  $h = 2^{-j}$ , corresponding to integer levels  $j = j_0, \dots, j_{\text{max}}$ .

In Section 4.1 we first propose one B-spline version of the common hierarchical approach for building adaptive approximations of a given data with prescribed error tolerance  $\varepsilon$ , and in Section 4.2 we suggest a local filter that makes the resulting adaptive approximations positivity-preserving, without noticeable loss of accuracy. In Section 4.3 we then describe a dynamic strategy to refine the particles in the course of their transport, so that the associated transport error is on the order of a (possibly different) prescribed tolerance  $\varepsilon'$ .

For notational simplicity we now label with  $j$  the objects that were previously labelled with their resolution  $h = 2^{-j}$ . For instance, we shall denote by

$$\varphi_{j,k}^n = \varphi_j(D_{j,k}^n(\cdot - x_{j,k}^n)),$$

the deformed particles from Equation (9) with resolution  $h = 2^{-j}$ , and so on.

#### 4.1 Adaptive approximations with multilevel B-splines

To build adaptive B-spline approximations of a given function  $g$ , we can apply the quasi-interpolation operator (12) in a hierarchical setting where significant approximations errors are corrected by localized layers of finer particles. Thus, starting from the coarse approximation  $g_{j_0} := A_{j_0}g$  we consider its successive corrections  $\sum_{k \in \mathbb{Z}^d} w_{j+1,k} \varphi_{j+1,k} := A_{j+1}(g - g_j)$ ,  $j = j_0, \dots, j_{\max}$ , where

$$g_j := \sum_{j'=j_0}^j \sum_{k \in \mathbb{Z}^d} w_{j',k} \varphi_{j',k} \quad (73)$$

denote the resulting approximations. Adaptivity is then classically obtained by selecting ‘‘significant’’ particles in this process. For instance, we may see small weights as negligible corrections, indeed discarding every particle  $\varphi_{j,k}$  for which

$$|w_{j,k}| \leq \zeta_j(\varepsilon) := 2^{-dj} \varepsilon ((2c_p)^d \|\varphi\|_{L^\infty})^{-1} \quad (74)$$

yields an error  $\|\sum_{k: |w_{j,k}| \leq \zeta_j(\varepsilon)} w_{j,k} \varphi_{j,k}\|_{L^\infty}$  that is bounded by  $\zeta_j(\varepsilon) 2^{dj} (2c_p)^d \|\varphi\|_{L^\infty} = \varepsilon$ . Moreover, we can restrict the above test to regions where the residual  $g - g_{j-1}$  has a chance to be significant. Specifically, we shall procede as follows (see Algorithm 4.1 below for a summary). Assume that for some  $j$  we have determined a domain  $\Omega_{j-1,+}$  where the residual has a chance to satisfy  $|g - g_{j-1}| > \varepsilon$ , and that we have gathered in a set  $K_{j,+}$  the indices of the level- $j$  particles needed for the correction on that domain, namely the  $k$ 's for which  $\Sigma_{j,k} := \text{supp}(\varphi_{j,k})$  overlaps  $\Omega_{j-1,+}$ . Then we can restrict the test (74) to those particles, and let  $K_j$  denote the resulting set of significant, i.e., selected particles. To find candidates  $K_{j+1,+}$  for the next level we only need to consider a domain  $\Omega_{j,+}$  that consists of (i) the supports of selected particles with  $k \in K_j$  (where the residual remains to be estimated), and (ii) the (possibly overlapping) part of  $\Omega_{j-1,+}$  where the residual  $g - g_{j-1}$  is actually measured above  $\varepsilon$ . Note that to determine this later part we can consider the cubes  $B_\infty(x_{j,k}, 2^{-j-1})$  with  $k \in K_{j,+}$  (which cover  $\Omega_{j-1,+}$ ), and estimate the approximation errors  $e_{j,k}^A = \|g - g_{j-1}\|_{L^\infty(B_\infty(x_{j,k}, 2^{-j-1}))}$  while computing the weights  $w_{j,k}$  involved in (74). Since level- $j$  B-splines are supported on cubes of radius  $2^{-j}c_p$ , see (10), this amounts in building  $K_{j+1,+}$  with respectively, every  $k' = 2k + l$  such that  $k \in K_j$  and  $\|l\|_\infty \leq 3c_p - 1$ , and every  $k' = 2k + l$  such that  $k \in K_{j,+}$  with  $e_{j,k}^A > \varepsilon$  and  $\|l\|_\infty \leq c_p$ . Let us summarize the resulting adaptive approximation operator  $A_\varepsilon$  as follows.

**Algorithm 4.1** (Adaptive particle approximation,  $A_\varepsilon : g \mapsto g_{j_{\max}} = \sum_{j=j_0}^{j_{\max}} w_{j,k} \varphi_{j,k}$ ).

1. At the coarsest level  $j_0$ , preactivate every particle (i.e., make it a candidate for a possible selection) by letting  $K_{j_0,+} := \mathbb{Z}^d$ .
2. Then for  $j = j_0, \dots, j_{\max}$ , compute and select the active particles as follows:
  - (a) for all  $k \in K_{j,+}$ , compute approximation weights  $w_{j,k}^A = w_{j,k}^A(g - g_{j-1})$  according to (12), and evaluate the local errors  $e_{j,k}^A = \|g - g_{j-1}\|_{L^\infty(B_\infty(x_{j,k}, 2^{-j-1}))}$ . Then select significant particles according to (74), i.e., let  $K_j := \{k \in K_{j,+} : |w_{j,k}^A| > \zeta_j(\varepsilon)\}$  and set

$$w_{j,k} := \begin{cases} w_{j,k}^A & \text{if } k \in K_j, \\ 0 & \text{otherwise;} \end{cases}$$

- (b) if  $j < j_{\max}$ , preactivate particles at the finer level for possible selection by letting
$$K_{j+1,+} := \{2k + l : k \in K_j, \|l\|_\infty \leq 3c_p - 1\} \cup \{2k + l : k \in K_{j,+}, e_{j,k}^A > \varepsilon, \|l\|_\infty \leq c_p\}$$
 (thus, adaptive regions at a given level are candidates for selection at the next level);
- (c) if the option is set, apply the positive correction filter (see Algorithm 4.2 below).

## 4.2 Positivity preserving hierarchical approximations

If the target function  $g$  is nonnegative, one may ask that its particle approximation is nonnegative as well. However, it is easily seen that the above scheme is likely to yield some negative weights. A first reason for this is that the single-level scheme (12) is not positive for  $p > 1$ . A second reason is due to the hierarchical framework: wherever  $g_{j-1}$  is below the target, the residual takes negative values which are likely to be approximated by negative level- $j$  particles.

The latter issue can be addressed by locally decreasing  $g_{j-1}$  in the neighborhood of a negative weight  $w_{j,k}$ , so as to increase the residual and hopefully correct the negativity of  $w_{j,k}$ . Since B-spline particles satisfy a scaling relation

$$\varphi_{j',k'} = \sum_{\|l\|_\infty \leq \frac{p+1}{2}} \sigma_l \varphi_{j'+1,2k'+l}, \quad (75)$$

it is possible to do so by refining coarse particles which contributions to  $\varphi_{j,k}$  will increase its weight. An attractive feature of such corrections is that they do not require new evaluations of the target function, or iterative approximations of updated residuals. Let us specify one such algorithm. Because it may be necessary to refine particles over several levels, it is useful to consider the multi-level scaling relations that one easily derives from (75),

$$\varphi_{j',k'} = \sum_{\|l\|_\infty \leq s_\delta} \sigma_l^{(\delta)} \varphi_{j'+\delta,2^\delta k'+l} \quad (76)$$

with multi-level refinement coefficients satisfying  $\sigma_l^{(\delta)} := \sum_{\|m\|_\infty \leq s_{\delta-1}} \sigma_m^{(\delta-1)} \sigma_{l-2m}^{(1)}$ ,  $s_\delta := 2s_{\delta-1} + 1$ , and initialized with  $\sigma^{(1)} = \sigma$ ,  $s_1 = \frac{p+1}{2}$ . Indeed, we can observe that if all the particles at the level  $j - \delta$ ,  $\delta \geq 1$ , were to be refined up to level  $j$ , the resulting increase to  $w_{j,k}$  would be

$$C_{j-\delta}(j, k) = \sum_{k' \in \mathbb{Z}^d} \sigma_{k-2^\delta k'}^{(\delta)} w_{j-\delta, k'}.$$

Therefore, we define the *correction level* associated to some given negative particle as

$$j_{\text{cor}}(j, k) := \begin{cases} \max \{j' < j : w_{j,k} + \sum_{j''=j'}^{j-1} C_{j''}(j, k) =: S_{j'}(j, k) \geq 0\} & \text{if } S_{j_0}(j, k) \geq 0, \\ j_0 & \text{otherwise.} \end{cases} \quad (77)$$

It corresponds to the coarser level from which neighboring particles should be refined in order to correct the weight  $w_{j,k}$ . Obviously, it is not necessary to refine *every* such coarse particle, since only those satisfying  $\|k - 2^\delta k'\|_\infty \leq s_\delta$  do contribute to  $(j, k)$ . Moreover, we do not need to *fully* refine them up to level  $j$ . Instead, the same increase to  $w_{j,k}$  can be obtained by refining them one level at a time, and only considering those contributing to  $(j, k)$  in the process, namely those  $(j', k')$  with  $\|2^{j-j'} k' - k\|_\infty \leq s_{j-j'}$ .

We note that these corrections are indeed local. However, we also observe that for  $p > 1$ , it may happen that some weights  $w_{j,k}$  remain negative after performing the above corrections. In this case we suggest to simply discard such weights  $w_{j,k}$ . Clearly, this can deteriorate the approximation accuracy, but in a hierarchical framework one can hope that finer layers of details will essentially correct the resulting errors. In practice we have indeed observed such a behavior, see Section 5.2. Let us now summarize the above correction filter, to be applied to the weights  $w_{j',k}$ ,  $j' = j_0, \dots, j$ , computed on step 2a of Algorithm 4.1. Note that here we compute the correction levels *before* refining the contributing particles so as not to break the possible symmetries in the particle grid.

**Algorithm 4.2** (Positive correction filter). *Let  $K_j^- := \{k \in K_j : w_{j,k} < 0\}$  denote the indices of the active particles to correct at level  $j$ . Then,*

1. if  $j > j_0$ ,
  - (a) set  $j_{\text{cor}}(j, k) < j$  as in (77), for all  $k \in K_j^-$ ;

- (b) then, refine every contributing particle. Namely, for all  $k \in K_j^-$  and all  $j' = j_{\text{cor}}(j, k), \dots, j-1$ , refine every particle  $(j', k')$  such that  $\|2^{j-j'}k' - k\|_\infty \leq s_{j-j'}$  by setting

$$w_{j'+1, 2k'+l} := w_{j'+1, 2k'+l} + \sigma_l w_{j', k'} \quad \text{for all } \|l\|_\infty \leq s_1, \quad \text{and} \quad w_{j', k'} := 0;$$

2. for all  $k \in K_j^-$ , set  $w_{j, k} := \max(0, w_{j, k})$ .

**Remark 4.3.** We observe that there is no need to preactivate further patches of finer particles for the next approximation level. Indeed the correction refinements on step (ii) do not change the approximation  $g_j$ , hence the residual. The only change to  $g_j$  occurs when discarding a negative weight  $w_{j, k}$ . There a significant error may be introduced, but since  $k \in K_j$  a finer patch is already preactivated, see step 2b of Algorithm 4.1.

### 4.3 Dynamic particle refinement without remapping

In order to achieve some prescribed accuracy  $\varepsilon'$  when transporting the multilevel particles

$$f_{j_{\max}}^n = \sum_{j=j_0}^{j_{\max}} \sum_{k \in \mathbb{Z}^d} w_{j, k}^n \varphi_j(D_{j, k}^n(\cdot - x_{j, k}^n)),$$

it is in general necessary to refine some of them over time. Indeed, the errors induced by the discrete transport operator will essentially depend on both their resolution level and the local smoothness of the flow, however at the initialization step their resolution only depends on the local smoothness of  $f^{\text{in}}$ . Furthermore, the flow may become suddenly less smooth in some regions, and finer particles will be needed there to maintain a constant accuracy. Therefore, rather than follow a conservative approach and automatically refine patches of particles to resolve the emerging features that may appear in the solutions, we decided to use the local error estimates from our previous error analysis to determine which particles are admissible for discrete transport, and which need to be refined. Given that both the number of levels and the number of overlapping particles per level are uniformly bounded, we have indeed  $\|(T^n - T_{\text{ex}}^n) f_{j_{\max}}^n\|_{L^\infty} \lesssim \sup_{j, k} \|w_{j, k}^n e_{j, k}^{n+1}\|_{L^\infty}$  hence a particle  $w_{j, k}^n \varphi_{j, k}^n$  will be said admissible for transport if it satisfies

$$|w_{j, k}^n \eta_{j, k}^n| \leq C_T \varepsilon', \quad (78)$$

where  $\eta_{j, k}^n$  is a computable estimate for the single-particle transport error  $\|e_{j, k}^{n+1}\|_{L^\infty}$  (see Appendix) and  $C_T$  is an ad-hoc constant, see Section 5.2.

We next observe that, although it is possible to represent exactly a deformed level- $j$  particle in terms of the finer ones with

$$\varphi_j(D_{j, k}^n(x - x_{j, k}^n)) = \sum_{\|l\|_\infty \leq c_p} \sigma_l \varphi_{j+1}(D_{j, k}^n(x - x_{j, k, l}^n)) \quad \text{with} \quad x_{j, k, l}^n = x_{j, k}^n + 2^{-j-1}(D_{j, k}^n)^{-1}l,$$

refining unadmissible particles in such a way can result in a dramatic increase of their total number. Assume indeed that every level- $j$  particle needs be refined in  $f^n$ . Since there is no reason why we should have  $D_{j, k}^n = D_{j, k'}^n$  and  $x_{j, k, l}^n = x_{j, k', l'}^n$  for  $k'$  and  $l'$  such that  $2k + l = 2k' + l'$ , replacing every  $\varphi_{j, k}^n$  by its exact finer representation is likely to add  $\sim 2^{dj}(2c_p + 1)^d$  new level- $(j+1)$  particles, which is much more than the particles involved by a uniform discretization at level  $j+1$ , and similar phenomena may happen on further time steps as well.

For that reason we propose instead to refine unadmissible particles  $\varphi_{j, k}^n$  in a “retroactive” fashion, by representing them in terms of the level- $(j+1)$  particles that would have been present in  $f^n$  if the original (structured)  $\varphi_{j, k}^0$  had been refined from the start. Note that some of those fine particles may already be present in  $f^n$ , and in such a case it suffices to update their weight. In particular, this approach allows to refer to any particle by its multilevel space-time indices without ambiguity: for all  $j, k, n$  we indeed have  $\varphi_{j, k}^n = \varphi_j(D_{j, k}^n(\cdot - x_{j, k}^n))$  with particle center and deformation matrix given by

$$x_{j, k}^n = F^{n-1}(x_{j, k}^{n-1}) = F^{n-1}(\dots F^0(x_{j, k}^0) \dots) \quad \text{and} \quad D_{j, k}^n = D_{j, k}^{n-1} J_{j, k}^{n-1} = \prod_{m=0}^{n-1} J_{j, k}^m \quad (79)$$

where  $x_{j,k}^0 = 2^{-j}k$ , and where  $J_{j,k}^m$  is computed as described in Section 3.3, see (38)-(39). Let us summarize our adaptive transport algorithm for multilevel particles as follows.

**Algorithm 4.4** ( $T_\varepsilon^n : f_{j_{\max}}^n \mapsto f_{j_{\max}}^{n+1}$ ). For  $j = j_0, \dots, j_{\max}$ , and then for  $k \in \mathbb{Z}^d$  such that  $w_{j,k}^n \neq 0$ ,

1. if  $j = j_{\max}$  or if the admissibility condition (78) is met, then the particle is transported by setting  $w_{j,k}^{n+1} = w_{j,k}^n$ ,  $x_{j,k}^{n+1} = F^n(x_{j,k}^n)$  and  $D_{j,k}^{n+1} = D_{j,k}^n J_{j,k}^n$  according to (37)-(39) ;
2. otherwise, it is dynamically refined by adding  $\sigma_l w_{j,k}^n$  to  $w_{j+1,2k+l}^n$  for  $\|l\|_\infty \leq \frac{p+1}{2}$  - which may involve the activation of new particles according to (79) - and finally setting  $w_{j,k}^n = 0$ .

**Remark 4.5.** A major drawback of the above strategy is the need to apply past numerical flows  $F^0, \dots, F^{n-1}$ , when refining particles at time step  $n$ . Alternative procedures involving local approximations of the flow  $F^n$  are currently being tested and will be addressed in a forthcoming article.

## 5 Numerical experiments

In this section we compare the numerical performances of the different particle methods in a computational domain  $\Omega = [0, 1]^2$ , using Leveque's swirling velocity field [22]

$$u_0(t, x) = -\sin^2(\pi x_0) \sin(2\pi x_1) g(t), \quad u_1(t, x) = \sin^2(\pi x_1) \sin(2\pi x_0) g(t) \quad (80)$$

with  $g(t) = \cos(\pi t / \tau)$ ,  $t \in [0, \tau]$ . The corresponding flow is easily pictured from the space pattern of  $u$  shown in Figure 1, and from the symmetry of  $g$  with respect to  $\tau/2$  which reverts the solutions to their initial state at  $t = \tau$ . We will take  $\tau = 2.5$  which corresponds to a moderate stretching at  $t = \tau/2$  (see Figures 2 and 4 below) and a fixed time step  $\Delta t = 0.025$ .

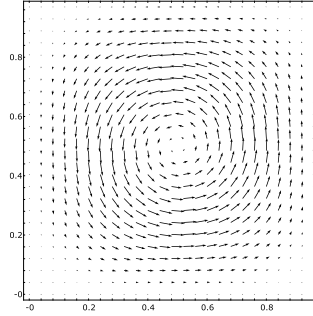


Figure 1: Leveque's swirling velocity field (80) at time  $t = 0$ .

Although the time symmetry may simplify the measure of the numerical errors, we note that by considering only the final accuracy one misses the intermediate errors resulting from the inaccurate transport of the particle shapes, which yields biased estimates for particle methods with no remappings. Therefore, we shall only make use of that feature in Section 5.2 when comparing the performances of the uniform and adaptive versions of the linearly transformed particle (LTP) scheme, with one remapping at least. In Section 5.1, where the traditional smoothed particle method (TSP) is compared to the forward semi-lagrangian (FSL) and the LTP schemes, we will only solve the equation on the half time interval  $[0, \tau/2]$ , and hence measure the numerical errors at the instant of maximal stretching, using a reference numerical solution obtained with substantially higher space and time resolution.

### 5.1 Numerical comparison of the TSP, FSL and LTP schemes

To compare the LTP scheme with the classical TSP and FSL methods reviewed in Section 2, we consider the two following cases.

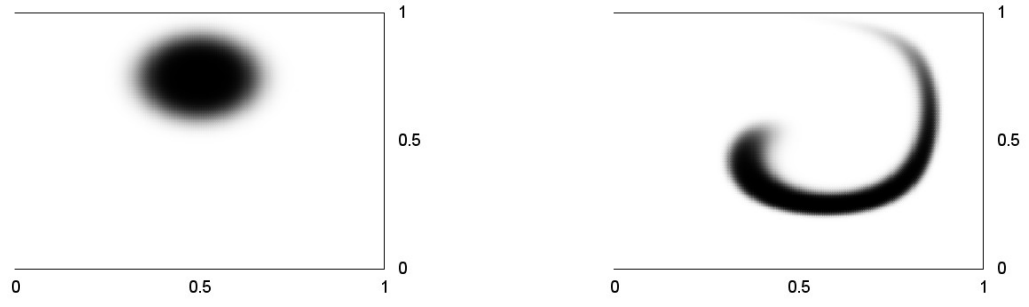


Figure 2: Solution profile at  $t = 0$  or  $\tau$  (left) and  $\tau/2$  (right) for the smooth hump (81).

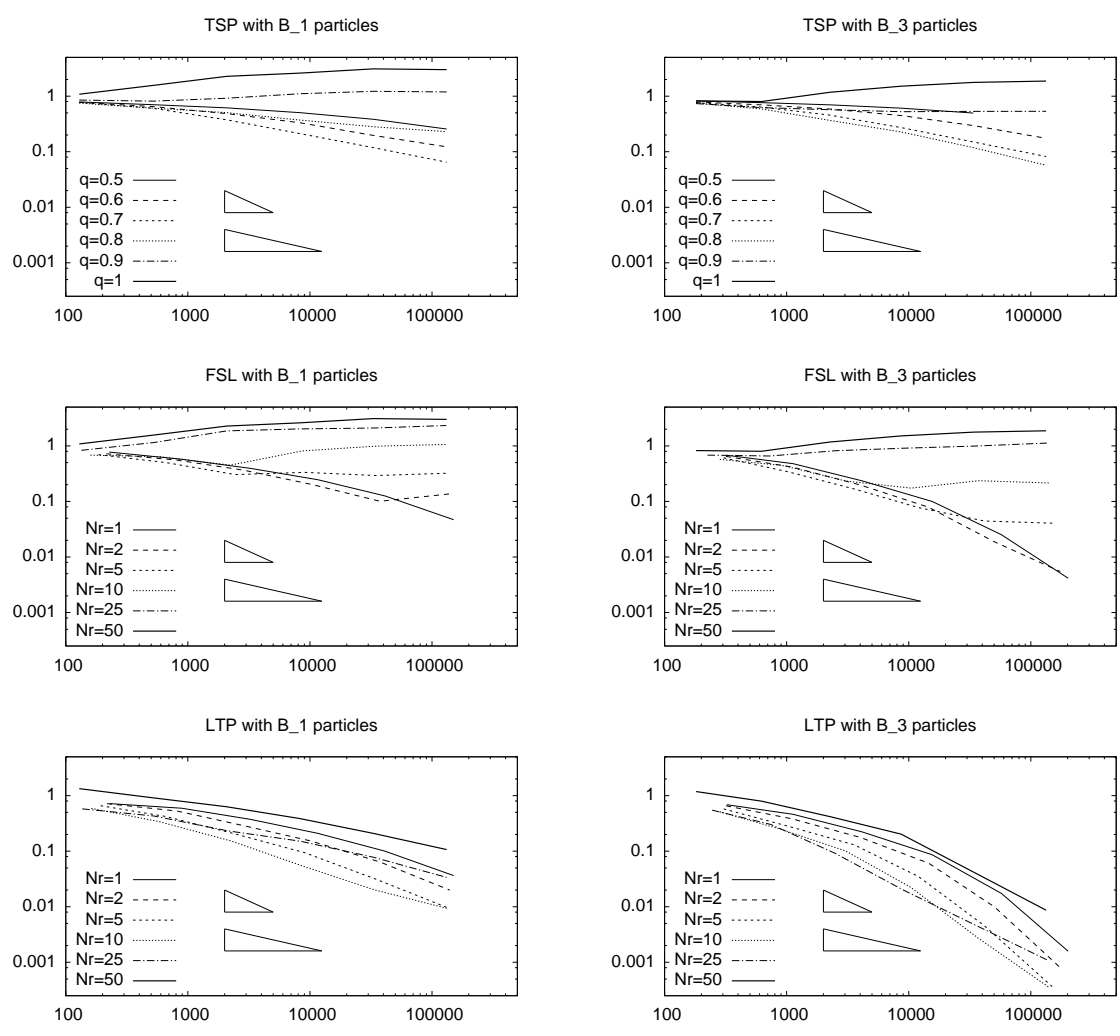


Figure 3: Convergence curves (relative  $L^\infty$  errors at  $t = \tau/2$  vs. average number of active particles) for the smooth hump test case shown in Figure 2, using the TSP, FSL and LTP schemes with B-spline particles of degree 1 and 3. Triangles represent slopes of 0.5 and 1,  $q$  is the overlapping exponent and  $N_r$  is the number of time steps between two remappings.

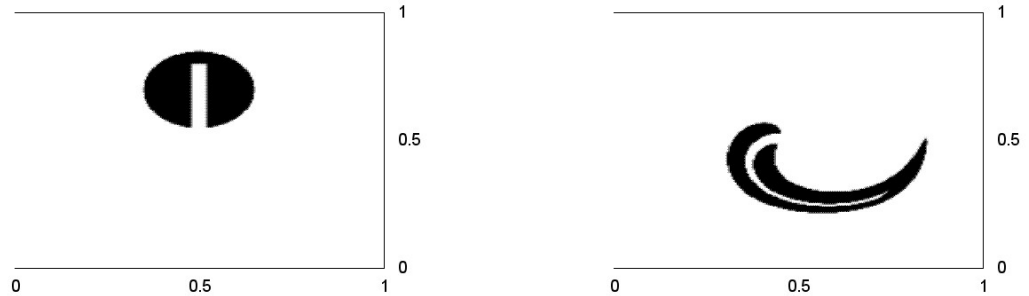


Figure 4: Solution profile at  $t = 0$  or  $\tau$  (left) and  $\tau/2$  (right) for the Zalesak's slotted disk (82).

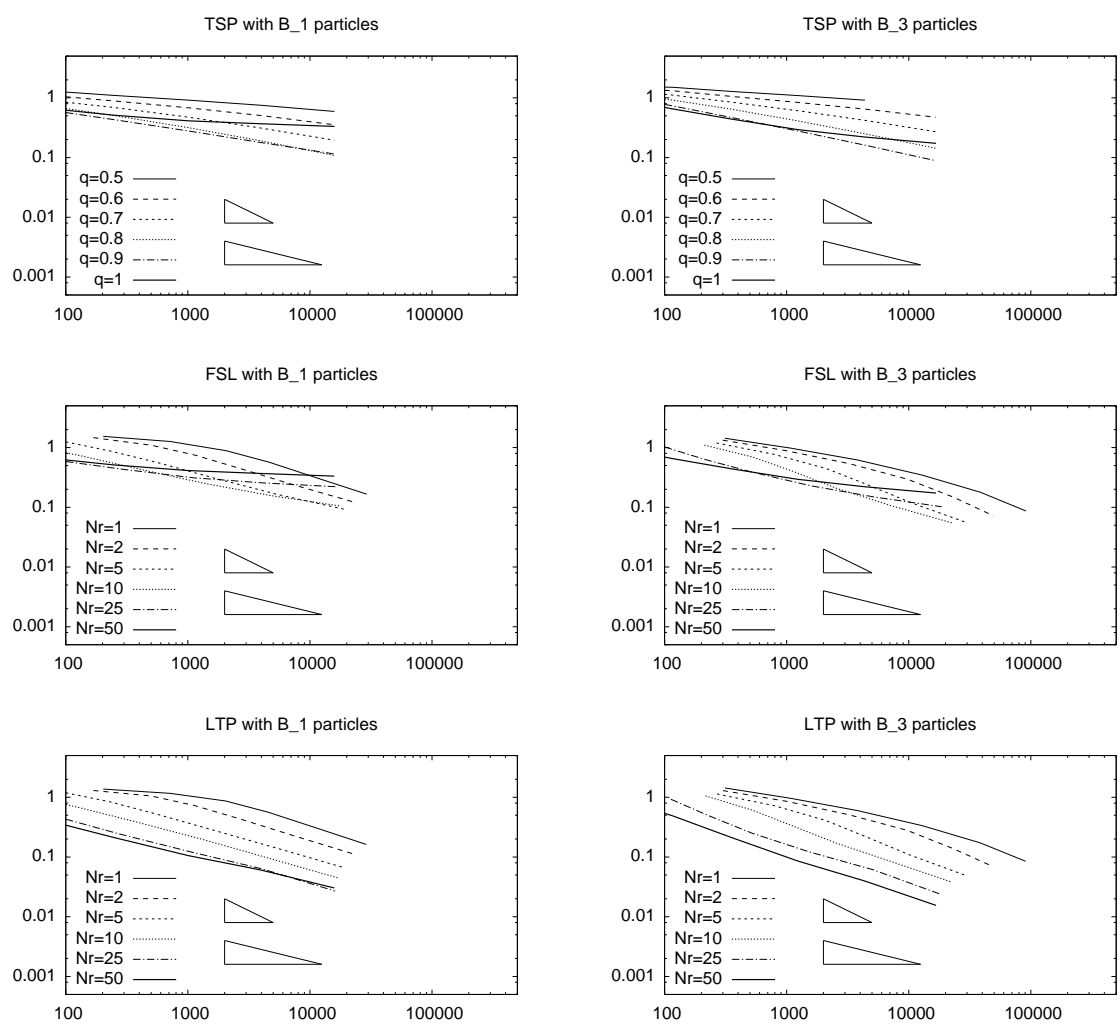


Figure 5: Convergence curves (relative  $L^1$  errors at  $t = \tau/2$  vs. average number of active particles) for the Zalesak's test case shown in Figure 4, using the TSP, FSL and LTP schemes with B-spline particles of degree 1 and 3. Triangles represent slopes of 0.5 and 1,  $q$  is the overlapping exponent and  $N_r$  is the number of time steps between two remappings.

- First, a smooth hump centered on  $(0.5, 0.75)$  given by

$$f^{\text{in}}(x) = \frac{1}{2} \left( 1 + \operatorname{erf} \left( a + b \sqrt{(x_0 - 0.5)^2 + (x_1 - 0.75)^2} \right) \right) \quad (81)$$

with  $a = 3.43$  and  $b = 21.43$ . Here  $\operatorname{erf}(s) = \frac{2}{\sqrt{\pi}} \int_0^s e^{-y^2} dy$  is the standard “error function” that smoothly spans  $[-1, 1]$ , see Figure 2.

- Second, a discontinuous Zalesak’s slotted disk of radius 0.15 centered on  $(0.5, 0.7)$

$$f^{\text{in}}(x) = H(0.15 - \sqrt{(x_0 - 0.5)^2 + (x_1 - 0.7)^2}) (1 - (1 - H(|x_0 - 0.5| - 0.02))(1 - H(x_1 - 0.8))) \quad (82)$$

where  $H(s) = \chi_{\{s \geq 0\}}$  denotes the Heaviside step function, see Figure 4.

In Figures 3 and 5 the relative errors are plotted versus the average number of active particles at  $t = \tau/2$ , in order to avoid a biased measure for the TSP method as explained above. For the smooth hump case we measure the errors in  $L^\infty$ , and for the discontinuous Zalesak disk we use the  $L^1$  norm. Here all three method have been run with B-spline particles with degree 1 or 3, initialized (and remapped, in the FSL and LTP cases) with the quasi-interpolation scheme (12) of corresponding order. For the TSP method we show the effect of varying the overlapping exponent  $q$  such that  $\epsilon = h^q$ , see Section 2.1, and for the FSL and LTP schemes we plot the runs corresponding to decreasing remapping frequencies, i.e., increasing values of the number  $N_r$  of time steps between two remappings. Observe that the higher  $q$  or  $N_r$ , the cheaper the simulations. In every set of curves we have used a thick line to emphasize the cheapest run: for the TSP scheme that corresponds to the case  $q = 1$  (particles radii are proportional to the initial meshsize) and for the FSL an LTP schemes that corresponds to the case with no remappings. In particular, we note that the FSL and TSP method coincide with such parameters. From these plots we make the following observations.

- First, we see that a necessary condition for the TSP method to converge is indeed that particles present an extended overlapping, i.e., the ratio  $\epsilon/h$  must go to  $\infty$  as  $h$  goes to 0. Moreover, the convergence is relatively slow, and it is not much improved by the use of third-order B-splines (although that helps in the cases of moderate particle overlapping,  $q \gtrsim 0.8$ ). This is not surprising since the theoretical convergence analysis requires vanishing moments for high-order accuracy, which the B-splines do not have.
- Again, our numerical tests confirm the announced necessary condition for the FSL scheme to converge: remapping frequency must be high. On the plus side, we note that on the smooth test case (81), the FSL scheme exhibits significantly higher convergence rates than the TSP method when  $B_3$  particles are used. However, to our view the method is severely hampered by the following dilemma: for values of  $N_r$  close to 1, problems with sharp edges such as the discontinuous Zalesak disk give rise to a strong numerical diffusion that can be seen (especially with  $B_3$  particles) from the increase of active particles and the deterioration of the accuracy ; decreasing the remapping frequencies helps reducing that effect, but doing so always leads to a loss of convergence (the lower the frequency, the sooner the stagnation).
- As expected from our analysis, the LTP scheme always converges including in the cheap, non-remapped runs. Moreover in the smooth case shown in Figure 3 the convergence rates are significantly higher than with the TSP method, and there the benefit of using  $B_3$  splines is obvious, just as in the FSL method. The striking result is that the loss of convergence observed in the FSL runs with low remapping frequencies is completely suppressed by the linear deformation of the particles.

## 5.2 Numerical study of an adaptive LTP scheme

To assess the ability of our adaptive particle strategy to improve the computational efficiency, we compare its convergence curves to those of the uniform LTP scheme, using the two following cases.

- First, the smooth hump (81) shown in Figure 2.

- Second, a smoothed version of the discontinuous Zalesak’s slotted disk shown in Figure 4, designed so as to get solutions of highly non uniform smoothness that still can be approximated in the supremum norm. Indeed our adaptive refinement strategies are aimed at balancing the local errors in the  $L^\infty$  norm, hence they have no reason to exhibit better convergence when the error is measured in another norm. The initial data  $f^{\text{in}}$  is then obtained by substituting the discontinuous Heaviside step function  $H(s) = \chi_{\{s \geq 0\}}$  in Equation (82) with its smooth approximation  $H_\epsilon(s) = \frac{1}{2}(1 + \text{erf}(s/\epsilon))$  corresponding to a transition zone with approximate diameter of  $4\epsilon$ . In the numerical tests we take  $\epsilon = 0.01$ .

In both cases, we thus plot the  $L^\infty$  convergence curves corresponding to the uniform LTP scheme using various values of  $N_r$  as above, and those obtained with our adaptive particle method using the optimal value observed in the uniform runs, namely  $N_r = 25$ . Since we now consider particle methods with at least one remapping step, numerical accuracy can be measured on the final time  $t = \tau$  where the exact solutions revert to their initial state. Here we have set the prescribed tolerances with  $\varepsilon' = \varepsilon$  (whose value varies along the curve) and fixed the constant  $C_T$  from Condition (78) to 2 to optimize the numerical performances. However we note that a proper study of how these parameters should be set in the general case remains to be done. As for the numerical estimate  $\eta_{j,k}^n$  involved in (78), after trying the various options described in the Appendix we have chosen to compute it with the first strategy, i.e., (86), with the simplification mentioned in Remark 5.1.

From Figure 6 we see that using adaptive particles with dynamic refinements yield a clear gain in terms of active particles. Moreover, in the Zalesak case where the numerical solutions are likely to strongly oscillate in the vicinity of the sharp edges, we also plot a series of runs obtained with our multilevel correction Algorithm 4.2 that enforces positive weights, hence positive particles. The resulting observation is that the numerical efficiency does not seem to suffer much from this local (and somewhat crude) positivity-preserving filter. To illustrate the behavior of the adaptive particle method, we also show on Figures 7 and 9 the distribution of active particle centers and associated level maps

$$j_{\text{map}}^n : x \mapsto \max \left\{ j : \sum_{k \in \mathbb{Z}^d} |w_{j,k}^n \varphi_{j,k}^n| \neq 0 \right\} \quad (83)$$

at  $t = \tau/2$ , corresponding to the adaptive runs that give the final error distributions displayed on Figures 8 and 10 for the hump and smoothed Zalesak initial data, respectively.

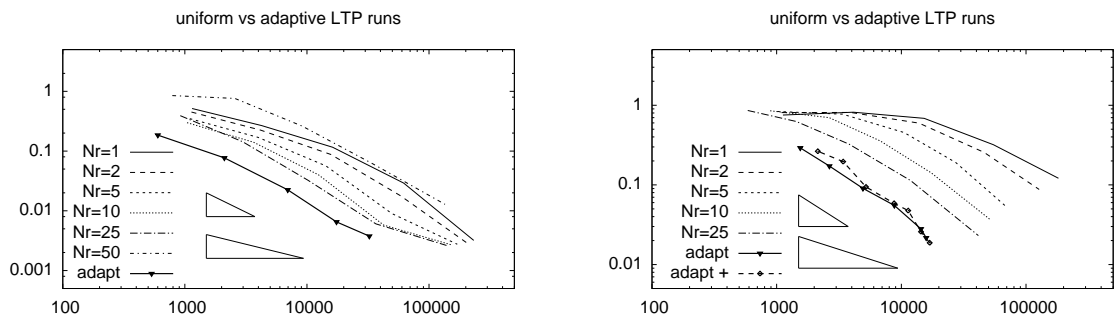


Figure 6:  $L^\infty$  convergence curves for the smooth hump (left) and the smoothed Zalesak’s slotted disk (right) cases in Leveque’s swirling flow. The relative  $L^\infty$  errors are plotted vs. the average number of particles. Triangles represent slopes of 0.5 and 1 and  $N_r$  is the number of time steps between two remappings.

Finally, we present one relevant feature of our adaptive particle scheme on Figures 8 and 10, showing the final error distributions obtained with uniform and adaptive runs using similar numbers of active particles for the hump and smoothed Zalesak initial data, respectively. In both cases we indeed observe that resorting to adaptive particles does not only reduce the maximum error, but it also balances its distribution over the computational domain, as it should be.

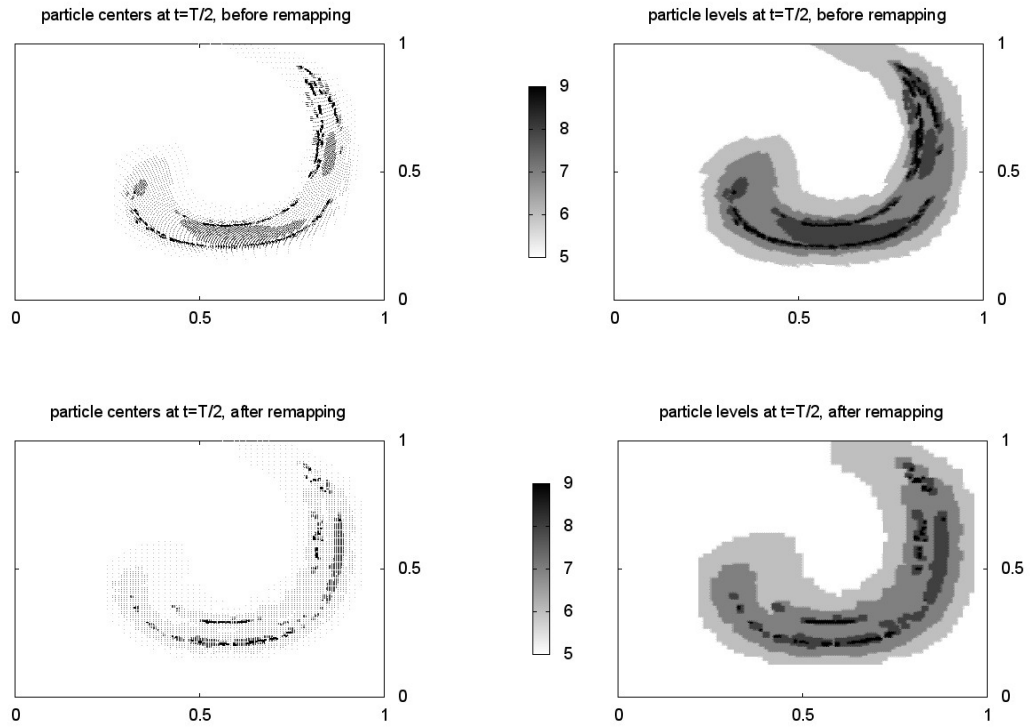


Figure 7: Particle centers (left) and level maps (right) at  $t = \tau/2$  for the smooth hump test case shown in Figure 2, before (top) and after (bottom) being remapped on a cartesian grid at  $t = \tau/2$ . Here we have used the same simulation parameters as in the adaptive runs shown in Figure 6, left, and a prescribed tolerance parameter  $\varepsilon$  set so as to get an average number of particles corresponding to a uniform run of level  $j = 7$ , see Figure 8 below.

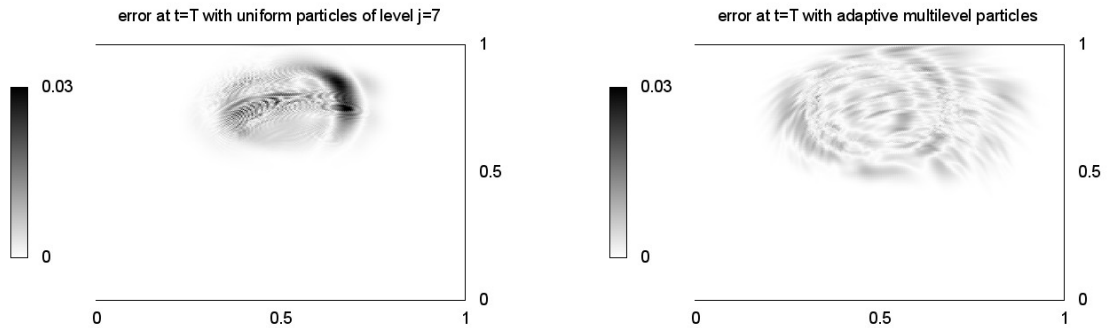


Figure 8: Final error distributions obtained for the smooth hump test case with a uniform run of level  $j = 7$  using about 10164 particles in average (left), and the adaptive run shown on Figure 7, using about 10498 particles in average (right).

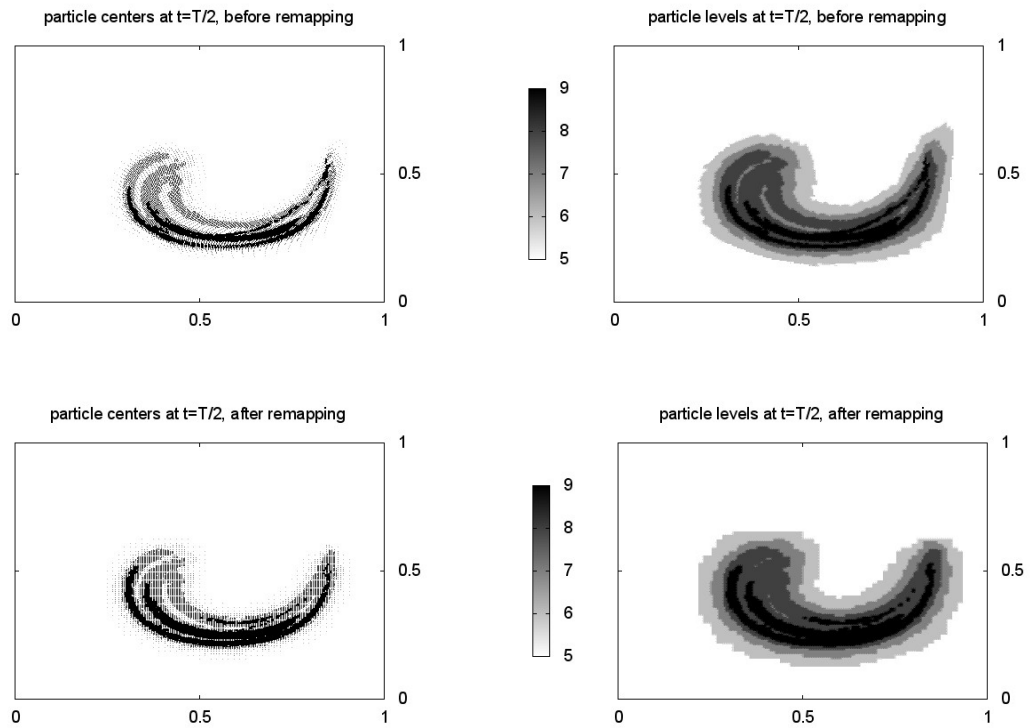


Figure 9: Particle centers (left) and level maps (right) for the smoothed Zalesak's slotted disk (see Figure 4), before (top) and after (bottom) being remapped on a cartesian grid at  $t = \tau/2$ . Here we have used the same simulation parameters as in the nonpositive adaptive runs shown in Figure 6, right, and a prescribed tolerance parameter  $\varepsilon$  set so as to get an average number of particles corresponding to a uniform run of level  $j = 7$ , see Figure 10 below.

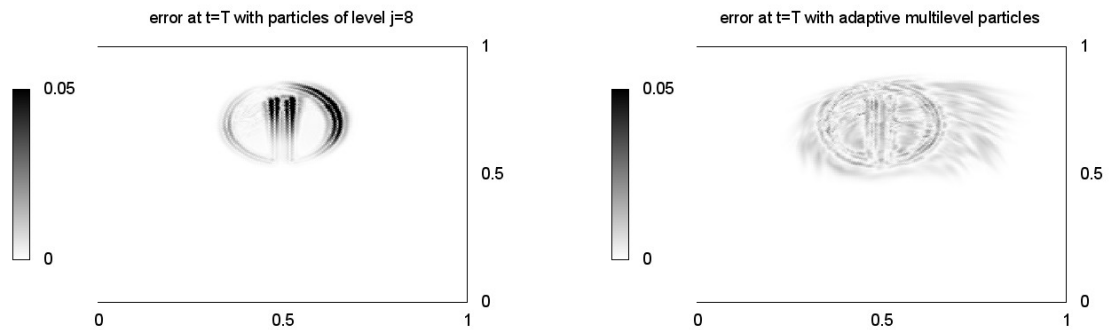


Figure 10: Final error distributions obtained for the smooth Zalesak's slotted disk with a uniform run of level  $j = 7$  using about 11864 particles in average (left), and the adaptive run shown on Figure 9, using about 11964 particles in average (right).

## Appendix: estimating the single particle transport error

To compute a practical estimate  $\eta_{j,k}^n$  for the local transport error involved in the admissibility condition (78), one can think of various approaches derived from our error analysis in Section 3.5.

- Inspired by the a priori bound (64), a first strategy consists of local estimates for the space derivatives of the velocity field  $u(t^n)$ .
- Based on the approximated Jacobian matrix  $J_{j,k}^n$ , a second strategy computes a direct estimate of the second line in (69).

Let us first describe the second strategy which is simpler. It consists in (i) replacing the supremum in (69) by a maximum over the stencil

$$F^n(x_{j,k,[\sigma,l]}^n) := F^n(x_{j,k}^n + (D_{j,k}^n)^{-1}(2^{-j}c_p\sigma e_l)), \quad \sigma \in \{-1, 1\}, \quad l = 1, \dots, d \quad (84)$$

that spans approximately  $F^n(\Sigma_{j,k}^n) \approx F_{\text{ex}}^n(\Sigma_{j,k}^n) \cup \Sigma_{j,k}^{n+1}$  (see Corollary 5.3 for an assessment of that claim), and (ii) using the numerical flow in place of the exact one. Thus, we set

$$\begin{aligned} \tilde{\eta}_{j,k}^n &:= \max_{\sigma,l} \|J_{j,k}^n(F^n(x_{j,k,[\sigma,l]}^n) - x_{j,k}^{n+1}) - (D_{j,k}^n)^{-1}(2^{-j}\sigma e_l)\|_\infty \\ &\approx \max_{\sigma,l} \|J_{j,k}^n(F^n(x_{j,k,[\sigma,l]}^n) - x_{j,k}^{n+1}) - ((F_{\text{ex}}^n)^{-1}(F^n(x_{j,k,[\sigma,l]}^n)) - x_{j,k}^n)\|_\infty \\ &\approx \sup_{x \in (\Sigma_{j,k}^{n+1} \cup F_{\text{ex}}^n(\Sigma_{j,k}^n))} \|J_{j,k}^n(x - x_{j,k}^{n+1}) - ((F_{\text{ex}}^n)^{-1}(x) - x_{j,k}^n)\|_\infty \end{aligned}$$

so that  $\eta_{j,k}^n := 2^{(d+1)j}|\varphi|_1 \|D_{j,k}^n\|_\infty \tilde{\eta}_{j,k}^n$  is a reasonable indicator for the local transport error.

The first strategy relies on finite difference approximations for the space derivatives

$$\Delta_l^j u(t)(x) = 2^j(u(t, x + 2^{-j-1}e_l) - u(t, x - 2^{-j-1}e_l)) \approx \partial_l u(t, x), \quad \Delta_{l_1, l_2}^j u(t) = \Delta_{l_1}^j(\Delta_{l_2}^j u(t)).$$

Thus, we mimic the local smoothness measures introduced in Lemma 3.5 and Corollary 3.6 with

$$\left\{ \begin{array}{l} |u|_{1, B_{j,k}^n}^* := \max_i \sum_l |\Delta_l^j u_i(t^n)(x_{j,k}^n)| \\ |u|_{2, B_{j,k}^n}^* := \max_i \sum_{l_1, l_2} |\Delta_{l_1, l_2}^j u_i(t^n)(x_{j,k}^n)| \end{array} \right\} \quad \left\{ \begin{array}{l} |u|_{1, \Sigma_{j,k}^n}^* := \max_i \sum_l \max_{\sigma,l} |\Delta_l^j u_i(t^n)(x_{j,k,[\sigma,l]}^n)| \\ |u|_{2, \Sigma_{j,k}^n}^* := \max_i \sum_{l_1, l_2} \max_{\sigma,l} |\Delta_{l_1, l_2}^j u_i(t^n)(x_{j,k,[\sigma,l]}^n)| \end{array} \right\}$$

(where the auxiliary nodes  $x_{j,k,[\sigma,l]}^n$  spanning  $\Sigma_{j,k}^n$  are given in (84)), and

$$\nu_{1,\omega}^{n,*} := |u|_{1,\omega}^* \exp(\Delta t |u|_{1,\omega}^*), \quad \nu_{2,\omega}^{n,*} := |u|_{2,\omega}^* \exp(\Delta t |u|_{1,\omega}^*) (1 + \Delta t \nu_{1,\omega}^{n,*}) \quad \text{with } \omega = B_{j,k}^n \text{ or } \Sigma_{j,k}^n.$$

The auxiliary  $\kappa$  coefficients are then set accordingly, with

$$\left\{ \begin{array}{l} \kappa_{1,(j,k)}^{n,*} := \nu_{1, B_{j,k}^n}^{n,*} + 2^{-j} d \alpha \\ \kappa_{2,(j,k)}^{n,*} := \frac{1}{2} \nu_{2, B_{j,k}^n}^{n,*} + d \alpha \end{array} \right\} \quad \left\{ \begin{array}{l} \kappa_{3,(j,k)}^{n,*} := 2d(1 + \Delta t \kappa_{1,(j,k)}^{n,*})^{d-1} \kappa_{2,(j,k)}^{n,*} \\ \kappa_{4,(j,k)}^{n,*} := d^2(1 + 2^{-j} \Delta t \kappa_{3,(j,k)}^{n,*})^2 (1 + \Delta t \kappa_{1,(j,k)}^{n,*})^{2(d-1)} \kappa_{2,(j,k)}^{n,*} \end{array} \right.$$

and following (65) we let

$$c_{j,k}^{e,n+1,*} := 2^{-j} \alpha + c_p \| (D_{j,k}^n)^{-1} \|_\infty \max \left\{ (1 + 2^{-j} \Delta t \kappa_{3,(j,k)}^{n,*})^{\frac{1}{d}} (1 + \Delta t \kappa_{1,(j,k)}^{n,*}), 1 + \Delta t \nu_{1, \Sigma_{j,k}^n}^{n,*} \right\} \approx c_{j,k}^{e,n+1}.$$

In order to compute an estimate for rhs in (64), it thus remains to find a numerical approximation for the backward flow term. One practical option is to see the domain  $F_{\text{ex}}^n(\Sigma_{j,k}^n)$  as a reasonable approximation of  $(\Sigma_{j,k}^{n+1} \cup F_{\text{ex}}^n(\Sigma_{j,k}^n))$ , and estimate in view of (51)

$$|(F_{\text{ex}}^n)^{-1}|_{2, (\Sigma_{j,k}^{n+1} \cup F_{\text{ex}}^n(\Sigma_{j,k}^n))} \approx |(F_{\text{ex}}^n)^{-1}|_{2, F_{\text{ex}}^n(\Sigma_{j,k}^n)} \leq \Delta t \nu_{2, \Sigma_{j,k}^n}^{n,*} \approx \Delta t \nu_{2, \Sigma_{j,k}^n}^{n,*}. \quad (85)$$

Thus, we may define

$$\eta_{j,k}^n := 2^{j(d-1)} \Delta t |\varphi|_1 \|D_{j,k}^n\|_\infty (c_{j,k}^{e,n+1,*} \kappa_{4,(j,k)}^{n,*} + (c_{j,k}^{e,n+1,*})^2 \nu_{2, \Sigma_{j,k}^n}^{n,*}) \quad (86)$$

as a computable approximation of the upper bound in (64).

**Remark 5.1.** *In practice the above estimate can be simplified by replacing the velocity smoothness measures  $|u_{i,\Sigma_{j,k}^n}^*$  with the pointwise quantities  $|u_{i,B_{j,k}^n}^*$ ,  $i = 1, 2$ . In our numerical tests indeed, we have not noticed any appreciable change when doing so.*

Let us end this section by observing that, although (85) may be sufficient in practice, it is possible to make it rigorous by using slight extensions  $\Sigma_{j,k}^{n,\lambda} := x_{j,k}^n + (D_{j,k}^n)^{-1}(B_\infty(0, 2^{-j}c_p(1+\lambda)))$  of the domain  $\Sigma_{j,k}^n \equiv \Sigma_{j,k}^{n,0}$ . Specifically, Lemma 5.2 below gives one sufficient condition on the extension parameter  $\lambda > 0$  for the following inequalities to hold true,

$$|(F_{\text{ex}}^n)^{-1}|_{2,(\Sigma_{j,k}^{n+1} \cup F_{\text{ex}}^n(\Sigma_{j,k}^n))} \leq |(F_{\text{ex}}^n)^{-1}|_{2,F_{\text{ex}}^n(\Sigma_{j,k}^{n,\lambda})} \leq \Delta t \nu_{2,\Sigma_{j,k}^{n,\lambda}}^n. \quad (87)$$

**Lemma 5.2.** *For  $\lambda \geq 0$ , we let  $\tilde{\Sigma}_{j,k}^{n+1,\lambda} := F_{\text{ex}}^n(x_{j,k}^n) + (J_{F_{\text{ex}}^n}(x_{j,k}^n))(D_{j,k}^n)^{-1}(B_\infty(0, 2^{-j}c_p(1+\lambda)))$  be an affine approximation of  $F_{\text{ex}}^n(\Sigma_{j,k}^{n,\lambda})$ . Then we have*

$$\tilde{\lambda} \geq 2^{-j} \Delta t L_1 \quad \implies \quad \Sigma_{j,k}^{n+1} \subset \tilde{\Sigma}_{j,k}^{n+1,\tilde{\lambda}} \quad (88)$$

$$\tilde{\lambda} \geq 2^{-j} \Delta t L_2 \quad \implies \quad F(\Sigma_{j,k}^n) \subset \tilde{\Sigma}_{j,k}^{n+1,\tilde{\lambda}} \quad (89)$$

$$\text{and } \lambda \geq \tilde{\lambda} + 2^{-j} \Delta t L_3(\tilde{\lambda}) \quad \implies \quad \tilde{\Sigma}_{j,k}^{n+1,\tilde{\lambda}} \subset F(\Sigma_{j,k}^{n,\lambda}) \quad (90)$$

with

$$L_1 := (1 + \Delta t \nu_{1,B_{j,k}^n}^n) \left[ \frac{\alpha}{c_p} + (1 + 2^{-j} \Delta t \kappa_{3,(j,k)}^n)^{-\frac{d+1}{d}} (1 + \Delta t \kappa_{1,(j,k)}^n)^d \kappa_{2,(j,k)}^n \| (D_{j,k}^n)^{-1} \|_\infty \right] \| D_{j,k}^n \|_\infty$$

$$L_2 := (1 + \Delta t \nu_{1,B_{j,k}^n}^n) \nu_{2,\Sigma_{j,k}^n}^n \frac{c_p}{2} \| (D_{j,k}^n)^{-1} \|_\infty^2 \| D_{j,k}^n \|_\infty$$

$$L_3(\tilde{\lambda}) := (1 + \Delta t \nu_{1,B_{j,k}^n}^n)^2 (\Delta t)^{-1} |(F_{\text{ex}}^n)^{-1}|_{2,\tilde{\Sigma}_{j,k}^{n+1,\tilde{\lambda}}} \frac{c_p}{2} (1 + \tilde{\lambda})^2 \| (D_{j,k}^n)^{-1} \|_\infty^2 \| D_{j,k}^n \|_\infty.$$

In particular, (87) holds as long as  $\lambda \geq 2^{-j} \Delta t (\max\{L_1, L_2\} + L_3(\tilde{\lambda}))$ , with  $\tilde{\lambda} = 2^{-j} \Delta t \max\{L_1, L_2\}$ .

As a consequence, it is possible to derive a rigorous versions of (85), involving the global smoothness measure  $\nu_2^n = \nu_{2,\mathbb{R}^d}^n$ , see Corollary 5.3. We shall also describe below a recursive algorithm for localizing this estimate.

*Proof.* For the sake of conciseness, we simplify the notations as in the proof of Lemma 3.3. For the first embedding we consider  $y \in \tilde{\Sigma}_\gamma$ , i.e.,  $y = \bar{x}_\gamma + J_\gamma^{-1} D_\gamma^{-1} z$  with  $\|z\| < 2^{-j} c_p$ , and observe that  $y \in \tilde{\Sigma}_\gamma^{\tilde{\lambda}}$  iff  $\|D_\gamma J_\gamma^{\text{ex}}(y - F_{\text{ex}}(x_\gamma))\|_\infty < 2^{-j} c_p(1 + \tilde{\lambda})$ . Now, we have

$$\begin{aligned} \|D_\gamma J_\gamma^{\text{ex}}(y - F_{\text{ex}}(x_\gamma))\|_\infty &\leq \|D_\gamma J_\gamma^{\text{ex}}(\bar{x}_\gamma - F_{\text{ex}}(x_\gamma))\|_\infty + \|D_\gamma J_\gamma^{\text{ex}} J_\gamma^{-1} D_\gamma^{-1} z\|_\infty \\ &\leq \|D_\gamma J_\gamma^{\text{ex}}\|_\infty e_{\Delta t}^n + \|z\|_\infty + \|D_\gamma J_\gamma^{\text{ex}}\|_\infty \| (J_\gamma^{\text{ex}})^{-1} - J_\gamma^{-1} \|_\infty \| D_\gamma^{-1} z \|_\infty \\ &< 2^{-j} c_p + 2^{-2j} \|D_\gamma\| \|F_{\text{ex}}\|_{1,B_\gamma} (2^{2j} e_{\Delta t}^n + \theta_\gamma^{-1-\frac{1}{d}} \mu_{1,\gamma}^d \mu_{2,\gamma} \|D_\gamma^{-1}\|_\infty c_p) \\ &< 2^{-j} c_p (1 + 2^{-j} \Delta t L_1) \end{aligned}$$

hence the first result. Turning next to (89), we now consider  $y \in \Sigma_\gamma$ , i.e.,  $y = x_\gamma + D_\gamma^{-1} z$  with  $\|z\| < 2^{-j} c_p$ , and observe that  $F_{\text{ex}}(y) \in \tilde{\Sigma}_\gamma^{\tilde{\lambda}}$  iff  $\|D_\gamma J_\gamma^{\text{ex}}(F_{\text{ex}}(y) - F_{\text{ex}}(x_\gamma))\|_\infty < 2^{-j} c_p(1 + \tilde{\lambda})$ . Using a Taylor expansion for  $s \mapsto F_{\text{ex}}(x_\gamma + s(y - x_\gamma))$ , we first write

$$\|F_{\text{ex}}(y) - F_{\text{ex}}(x_\gamma) - (J_\gamma^{\text{ex}})^{-1}(y - x_\gamma)\|_\infty < \frac{1}{2} \|F_{\text{ex}}\|_{2,\Sigma_\gamma} (2^{-j} c_p \|D_\gamma^{-1}\|_\infty)^2 \leq 2^{-2j} \Delta t \frac{\nu_{2,\Sigma_\gamma}}{2} (c_p \|D_\gamma^{-1}\|_\infty)^2.$$

It follows that

$$\begin{aligned} \|D_\gamma J_\gamma^{\text{ex}}(F_{\text{ex}}(y) - F_{\text{ex}}(x_\gamma))\|_\infty &\leq \|z\|_\infty + \|D_\gamma J_\gamma^{\text{ex}}\|_\infty \|F_{\text{ex}}(y) - F_{\text{ex}}(x_\gamma) - (J_\gamma^{\text{ex}})^{-1}(y - x_\gamma)\|_\infty \\ &< 2^{-j} c_p (1 + 2^{-j} \Delta t \|D_\gamma\| (1 + \Delta t \nu_{1,B_\gamma}^n) \frac{c_p}{2} \nu_{2,\Sigma_\gamma} \|D_\gamma^{-1}\|_\infty^2) \end{aligned}$$

hence the second embedding. For the last one, we take  $y \in \tilde{\Sigma}_\gamma^{\tilde{\lambda}}$ , i.e.,  $y = F_{\text{ex}}(x_\gamma) + (J_\gamma^{\text{ex}})^{-1} D_\gamma^{-1}(z)$  with  $\|z\|_\infty < 2^{-j} c_p(1 + \tilde{\lambda})$ , and observe that  $\tilde{\Sigma}_\gamma^{\tilde{\lambda}} \subset F_{\text{ex}}(\Sigma_\gamma^{\tilde{\lambda}})$  iff  $\|D_\gamma(F_{\text{ex}}^{-1}(y) - x_\gamma)\|_\infty < 2^{-j} c_p(1 + \tilde{\lambda})$ .

Using that  $\tilde{\Sigma}_\gamma^\lambda \subset B_\infty(F_{\text{ex}}(x_\gamma), 2^{-j}c_p(1+\tilde{\lambda}))\|(D_\gamma J_\gamma^{\text{ex}})^{-1}\|_\infty$ , we now write with a Taylor expansion of  $s \mapsto F_{\text{ex}}^{-1}(F_{\text{ex}}(x_\gamma) + s(y - F_{\text{ex}}(x_\gamma)))$  that

$$\|F_{\text{ex}}^{-1}(y) - x_\gamma - J_\gamma^{\text{ex}}(y - F_{\text{ex}}(x_\gamma))\|_\infty < \frac{1}{2}|F_{\text{ex}}^{-1}|_{2, \tilde{\Sigma}_\gamma^\lambda}(2^{-j}c_p(1+\tilde{\lambda}))\|(D_\gamma J_\gamma^{\text{ex}})^{-1}\|_\infty^2.$$

It follows that

$$\begin{aligned} \|D_\gamma(F_{\text{ex}}^{-1}(y) - x_\gamma)\|_\infty &\leq \|z\|_\infty + \|D_\gamma(F_{\text{ex}}^{-1}(y) - x_\gamma - J_\gamma^{\text{ex}}(y - F_{\text{ex}}(x_\gamma)))\|_\infty \\ &< 2^{-j}c_p(1+\tilde{\lambda} + 2^{-j}\|D_\gamma\|_\infty|F_{\text{ex}}^{-1}|_{2, \tilde{\Sigma}_\gamma^\lambda} \frac{c_p}{2} [(1+\tilde{\lambda})\|D_\gamma^{-1}\|_\infty(1+\Delta t\nu_{1, B_\gamma})]^2), \end{aligned}$$

hence the final result.  $\square$

Because the above result also involves a local smoothness measure of the backward flow, it is not directly applicable to find the optimal extension parameter  $\lambda_{\text{opt}} = 2^{-j}\Delta t(\max\{L_1, L_2\} + L_3(\tilde{\lambda}))$ . However, it gives a first estimate based on the global smoothness measure of  $u$ , which can be refined recursively as follows.

**Corollary 5.3.** *Let  $\tilde{\lambda} := 2^{-j}\Delta t\|D_{j,k}^n\|_\infty \max\{L_1, L_2\}$  and define*

$$\lambda^{(0)} := \tilde{\lambda} + 2^{-j}\Delta t\|D_{j,k}^n\|_\infty L_3^{(0)} \quad \text{with} \quad L_3^{(0)} := \frac{1}{2}\nu_{2, \Sigma_{j,k}^n}^n(1 + \Delta t\nu_{1, B_{j,k}^n}^n)^2(1 + \tilde{\lambda})^2\|(D_{j,k}^n)^{-1}\|_\infty^2 \geq L_3(\tilde{\lambda}).$$

Then we have

$$|(F_{\text{ex}}^n)^{-1}|_{2, \langle \Sigma_{j,k}^{n+1} \cup F_{\text{ex}}^n(\Sigma_{j,k}^n) \rangle} \leq |(F_{\text{ex}}^n)^{-1}|_{2, \tilde{\Sigma}_{j,k}^{n+1, \tilde{\lambda}}} \leq |(F_{\text{ex}}^n)^{-1}|_{2, F_{\text{ex}}^n(\Sigma_{j,k}^{n, \lambda^{(0)}})} \leq \Delta t\nu_{2, \Sigma_{j,k}^n}^n. \quad (91)$$

Moreover, it is possible to improve the above estimate. We have indeed

$$L_3(\tilde{\lambda}) \leq L_3^{(1)} := \frac{1}{2}\nu_{2, \Sigma_{j,k}^{n, \lambda^{(0)}}}^n c_p(1 + \Delta t\nu_{1, B_{j,k}^n}^n)^2(1 + \tilde{\lambda})^2\|(D_{j,k}^n)^{-1}\|_\infty^2 \leq L_3^{(0)},$$

so that (91) holds with  $\lambda^{(1)} := \tilde{\lambda} + 2^{-j}\Delta t\|D_{j,k}^n\|_\infty L_3^{(1)} \leq \lambda^{(0)}$ , and this argument can be carried out recursively to improve the resulting estimates of  $|(F_{\text{ex}}^n)^{-1}|_{2, \langle \Sigma_{j,k}^{n+1} \cup F_{\text{ex}}^n(\Sigma_{j,k}^n) \rangle}$ .

## 6 Conclusion and further work

We have introduced a formal class of particle methods for transport problems with high-order polynomial deformations, and established the convergence of an explicit LTP scheme for the first-order case. Our preliminary numerical results demonstrate the improved convergence of the LTP scheme compared to the traditional ‘‘smoothed’’ particle method (TSP) with extended overlapping, as well as the need of lower remapping frequencies compared to the FSL scheme, leading to lower numerical diffusion and computational costs. On a practical level we emphasize that implementing the FSL scheme is made simple by the fact that it only involves pointwise evaluations of the numerical forward flow, a numerical object at the core of any particle scheme. We also note that for computational efficiency of algorithms involving pointwise evaluation of the numerical solutions (e.g., remapping or plotting routines) one may want to first localize the particles in a logical mesh. For that purpose one can use the criterion given in Section 3.4.

In a near future we shall develop methods to deal with non-linear transport problems arising, e.g., in plasma models, and further investigate the properties of our adaptive multilevel scheme.

## Acknowledgments

The author thanks Eric Sonnendrücker, Albert Cohen, Jean-Marie Mirebeau and Jean Roux for fruitful discussions. Most of this work has been carried out while the author was Fulbright visiting scholar at the Lawrence Berkeley National Laboratory with partial support from the France-Berkeley Fund, and fruitful interactions with Alex Friedman, Steve Lund, Dave Grote and John Verboncoeur are gratefully acknowledged.

## References

- [1] F. Assous, T. Pougéard Dulinbert and J. Segré, *A new method for coalescing particles in PIC codes*, J. Comp. Phys. 187, 550–571, 2003.
- [2] W.B. Bateson and D.W. Hewett, *Grid and particle hydrodynamics: beyond hydrodynamics via fluid-element particle-in-cell*, J. Comp. Phys. 144, 358–378, 1998.
- [3] J.T. Beale and A. Majda *Vortex methods II: Higher order accuracy in two and three dimensions*, Math. Comp. 32, 29–52, 1982.
- [4] R. Bellman, *The stability of solutions of linear differential equations*, Duke Math. J. 10, 643–647, 1943.
- [5] M. Bergdorf, G.-H. Cottet and P. Koumoutsakos, *Multilevel adaptive particle methods for convection-diffusion equations* Multiscale Model. Simul. 4, 328–357, 2005.
- [6] M. Bergdorf and P. Koumoutsakos, *A lagrangian particle-wavelet method* Multiscale Model. Simul. 5, 980–995, 2006.
- [7] C.K. Birdsall and A.B. Langdon, *Plasma physics via computer simulation*, McGraw-Hill, New York, 1985.
- [8] A.J. Chorin, *Numerical study of slightly viscous flow*, J. Fluid Mech. 57, 785–796, 1973.
- [9] C. Chui and H. Diamond, *A Characterization of Multivariate Quasi-interpolation Formulas and its Applications*, Numer. Math. 57, 105–121, 1990.
- [10] A. Cohen and B. Perthame, *Optimal approximation orders for transport equations with pseudo-particle methods*, SIAM J. Math. Anal. 32, 616–636, 2000.
- [11] C.J. Cotter, J. Frank and S. Reich, *The remapped particle-mesh semi-Lagrangian advection scheme*, Q. J. Meteorol. Soc. 133, 251–260, 2007.
- [12] G.-H. Cottet and P.D. Koumoutsakos, *Vortex methods. Theory and practice*, Cambridge University Press, Cambridge, 2000.
- [13] G.-H. Cottet, P. Koumoutsakos and M.L.O. Salihi, *Vortex methods with spatially varying cores*, J. Comp. Phys. 162, 164–85, 2000.
- [14] N. Crouseilles, T. Respaud and E. Sonnendrücker, *A forward semi-Lagrangian method for the numerical solution of the Vlasov equation*, Comp. Phys. Comm. 180, 1730–1745, 2009.
- [15] C. de Boor, *A Practical Guide to Splines*, Springer-Verlag, 1978.
- [16] J. Denavit, *Numerical simulation of plasmas with periodic smoothing in phase space*, J. Comp. Phys. 9, 75–98, 1972.
- [17] R.A. DeVore, *Nonlinear approximation*, Acta Numerica 7, 51–150, Cambridge Univ. Press, 1998.
- [18] R.T. Glassey, *The Cauchy problem in kinetic theory*, SIAM, Philadelphia, 1996.
- [19] D.W. Hewett *Fragmentation, merging, and internal dynamics for PIC simulation with finite size particles*, J. Comp. Phys. 189, 390–426, 2003.
- [20] T. Hou *Convergence of a variable blob vortex method for the Euler and Navier-Stokes equations*, SIAM J. Numer. Anal. 27, 1387–1404, 1990.
- [21] G. Lapenta, *Particle Rezoning for Multidimensional Kinetic Particle-In-Cell Simulations*, J. Comp. Phys. 181, 317–337, 2002.
- [22] R.J. Leveque, *High-resolution conservative algorithms for advection in incompressible flow*, SIAM J. Numer. Anal., 33, 627–665, 1996.

- [23] R.D. Nair, J.S. Scroggs and F.H.M. Semazzi, *A forward-trajectory global semi-Lagrangian transport scheme*, J. Comp. Phys. 190, 275–294, 2003.
- [24] Rasio F. *Particle methods in astrophysical fluid dynamics*, Prog. Theo. Phys. Suppl., 138, 609–621, 2000.
- [25] P.A. Raviart, *An analysis of particle methods*, Numerical methods in fluid dynamics (Como, 1983), 243–324, Lecture Notes in Math., 1127, Springer, Berlin, 1985.
- [26] Z.-H. Teng, L.-A. Ying and P. Zhang *Convergence of the variable-elliptic-vortex method for Euler equations*, SIAM J. Numer. Anal. 32, 754–774, 1995.
- [27] M. Unser and I. Daubechies, *On the approximation power of convolution-based least squares versus interpolation*, IEEE Trans. Sig. Proc., 45 (7), 1697–1711, July 1997.
- [28] B. Wang, G. H. Miller and P. Colella, *A Particle-In-Cell method with adaptive phase-space remapping for kinetic plasmas*, Submitted for publication, 2010.